AN ABSTRACT OF THE THESIS OF

Katy L. Schwinghamer for the Master of Science

in Physical Sciences presented on May 18, 2017

Title: The Origin of High Silica and Low pH in the Groundwater of the Quaternary Terrace Deposits in the Northern Khorat Basin in Northeastern Thailand

Thesis Chair: Dr. Marcia Schulmeister

Abstract approved: _____

The groundwater of the Khorat Plateau in Northeastern Thailand is used as a water resource due to its excellent quality. The region is underlain by an aquifer system consisting of two zones separated by a clay lens. The system is composed of unconsolidated sediments that contain different forms (crystalline, cryptocrystalline, and amorphous) of silica-bearing rocks and minerals. The sediments are overlain by highly weathered, laterite soils that allow for rapid recharge to the aquifer system, with subsequent lateral flow. Dissolved silica concentrations (10-68 mg/L SiO_2) in some aquifer depths are higher than normally observed in natural environments (35 mg/L SiO_2). The system also contains unusually low pH values, as low as 4.6, which may result from the formation of silicic acid resulting from silica dissolution and a lack of a buffering capacity in the system. To evaluate this hypothesis, the saturation indices of silica minerals were determined along a groundwater flow gradient, and modeling was conducted to observe how the water changes as it moves along the flow path. Saturation indices generally increased down gradient for crystalline, cryptocrystalline, and amorphous silica materials, demonstrating increasing dissolved silica concentrations.

Different saturation index values for the three silica forms indicate the conditions for dissolution of amorphous silica and precipitation of crystalline silica existing in all locations down the flow path. The conditions for dissolution exist in upgradient wells and precipitation in mid- and downgradient wells for cryptocrystalline silica. This suggests the dissolution of amorphous and cryptocrystalline silica have contributed to the dissolved silica concentrations. Dissolved silica, alkalinity and pH trends indicate that as silica concentrations spike, pH values decrease suggesting the possible formation of silicic acid. Low alkalinity concentrations and pH values in some parts of the aquifer system suggest the lack of a buffer zone in these locations.

Keywords: groundwater, chemistry, geology, silica, pH, dissolution

THE ORIGIN OF HIGH SILICA AND LOW PH IN THE GROUNDWATER OF THE QUATERNARY TERRACE DEPOSITS IN THE NORTHERN KHORAT BASIN IN NORTHEASTERN THAILAND

A Thesis

Presented to

The Department of Physical Sciences

EMPORIA STATE UNIVERSITY

In Partial Fulfillment

of the Requirements for the Degree

Master of Science

By

Katy Lee Schwinghamer

May 18, 2017

Dr. Marcia Schulmeister, Committee Chair

Dr. Rungrung Lertsirivorakul, Committee Member

Dr. Carlos Peroza, Committee Member

Dr. Kim Simons, Department Chair

Dr. Jerry Spotswood, Dean of the Graduate School and Distance Education

ACKNOWLEDGMENTS

I would like to thank and acknowledge my advisor, Dr. Marcia Schulmeister, for her support, encouragement, and guidance throughout my academic career. I would also like to thank my committee members, Dr. Rungruang Lertsirivorakul, and Dr. Carlos Peroza, for their time and participation in my graduate research.

I would like to express my gratitude to the graduate students, Biw, Gao, Somo, Samart, and Kittya, in the Department of Geotechnology at Khon Kaen University for their time and effort in completing field and lab work necessary to complete this research. Your assistance is greatly appreciated.

I would like to thank the faculty of the Earth Science and Chemistry departments at Emporia State University for their contributions throughout my time at Emporia State University. Your knowledge and support have been greatly beneficial to the completion of my college degrees.

Lastly, I would like to thank my family for their love and support throughout my educational career. Without you, I would not be where I am today.

TABLE OF CONTENTS

LIST OF APPENDICES

LIST OF TABLES

LIST OF FIGURES

CHAPTER 1: STATEMENT OF PROBLEM AND OBJECTIVES

1.1 Introduction

The aquifers of the Khorat Plateau lie in alluvial and colluvial deposits containing silica-bearing rocks and minerals. They provide good quality groundwater that is utilized as a water resource for Northeastern Thailand. Protection of these waters is essential due to their agricultural, municipal, and domestic uses as an alternative to unreliable surface waters during drought. The climate of the region has a characteristic rainy and wet season in which approximately 80% of the annual rainfall falls during the rainy season. Dissolved silica concentrations (10-60 mg/L SiO_2) in groundwater in some areas of the Khorat Plateau are higher than normally found in natural waters, 35 mg/L SiO_2. Additionally, pH values have been routinely low in the area, with values as low as 4.6 (Thana Thoranee Co. Ltd., 2013). High silica concentrations can cause scaling of machinery while pH values lower than 6.5 can cause corrosion (McFarland et al., 2008). The origin of these conditions has yet to be explained.

The highest dissolved silica concentrations and lowest pH values have been recorded in flowing artesian wells located in the terrace gravel deposits of the Khorat Plateau. They may be attributed to the silicic acid formation resulting from rapid chemical weathering of silica materials in response to high infiltration rates from permeable soils. This thesis will test the hypothesis that silica-bearing rocks and minerals present in the aquifer matrix are contributing to the high concentrations of dissolved silica, as well as the acidic environment, found in the groundwater system. To test this hypothesis, groundwater samples were collected and a laboratory analysis of major ion and silica concentrations and pH were conducted. Parameters obtained in the field were

used along with the laboratory results to identify the saturation index values of silica minerals. Trends were examined, using new and previously obtained data, to determine how the water chemistry varied along an established groundwater flow path.

1.2 Objectives

1. To identify spatial and temporal variations in major ions, silica, and pH within terrace gravels. To meet this objective, historical chemical analyses obtained in 2011-2012 by the Thailand Department of Groundwater Resources and new data collected as a part of this study were examined in wells located at various points along established flow paths.

2. To identify spatial and temporal variations in the saturation state of various silica species at the site. Saturation index values for three forms of silica were determined based on field and lab data from the sampled wells.

3. To identify spatial and temporal variations in pH and its possible relationship to silica concentrations. To do this, seasonal and gradient trends were evaluated utilizing field and chemical data to determine how groundwater reacted as it moved along the flow gradient.

CHAPTER 2: BACKGROUND

2.1 Silica in the Environment

Silica materials make up approximately 90% of Earth's crust (Tarbuck and Lutgens, 2015). Silica can exist in nature with different internal structures of the silica dioxide molecules. Crystalline silica minerals, such as quartz, have an ordered internal structure that forms crystals that can be seen with the naked eye. Polycrystalline silica rocks, such as chalcedony, chert, and jasper, contain many tiny crystals that must be viewed under special microscopic conditions. The structure of these rocks vary depending on how ordered internal arrangement is. Amorphous silica rocks contain no order in their internal structures (Krauskopf, 1959).

When a silica solid reacts with water, it forms a weak acid, silicic acid, as demonstrated in the following equation.

$$SiO_2(s) + 2H_2O(l) \leftrightarrow H_4SiO_4(aq)$$

Silica dissolution is dependent on internal crystalline structure, temperature of the solution, and pH of the solution. Due to strong intermolecular forces that bind their ordered internal molecular structures, crystalline silica minerals are relatively insoluble in natural water conditions with a solubility of 6-11 ppm at 25°C. Amorphous silica rocks have a much higher solubility, 110-140 at 25°C, due to their disordered molecular structure (Krauskopf, 1959). Polycrystalline rocks have a solubility depended on amount of order in the internal structure. A more ordered structure indicates larger crystals and a lower solubility. In high temperature environments and in alkaline environments, silica solubility increases.

The presence of dissolved silica in groundwater is an indication of the chemical weathering of silica minerals as well as groundwater circulation conditions (Pradeep et al., 2016). High dissolved silica concentrations have been observed on the consolidated and unconsolidated aquifers of the Khorat Plateau since the 1950s (LaMoreaux et al., 1958). Silica values as high as 200 mg/L SiO_2 were recorded in waters of bedrock aquifers (Haworth, 1966), and values as high as 66.7 mg/L SiO_2 were observed in unconsolidated aquifers (Thana Thoranee Co. Ltd., 2013).

2.1.1 Controls on Silica Dissolution

Silica dissolution is dependent on solution pH and temperature as well as the form of silica mineral (Krauskopf, 1959). Silica exists in the solid state as silica dioxide, SiO_2. When SiO_2 reacts with water, it forms a weak acid called silicic acid. Silica solubility increases as temperature increases and in alkaline environments. Silica solids can exist in different forms dependent on their internal molecular structure. Three forms have been identified in the alluvial sediments: crystalline, polycrystalline, and amorphous. Crystalline silica minerals contain an internal structure in which the silica dioxide molecules are ordered and crystals can be seen with the naked eye. Crystalline forms of silica are nearly insoluble in the natural water system, with a solubility of between 6-11 ppm at 25°C and exist in the groundwater system as quartz (Krauskopf, 1959). Amorphous silica rocks lack an internal molecular structure and are the most soluble form with a solubility ranging from 100-140 ppm at 25°C (Krauskopf, 1959). Amorphous silica is found on site in the form of tektites, or natural glass formed from impacts of meteorites, and petrified wood. Polycrystalline silica rocks contain extremely small crystals and have a solubility in between that of the amorphous and crystalline forms that

varies depending the extent of order in the internal structure. Polycrystalline silica rocks in the alluvial deposits include chert, jasper, and chalcedony.

2.2 Geomorphic Setting of the Khorat Plateau

The Khorat Plateau covers an area of over 150,000 km^2 in northeastern Thailand (Haworth et el., 1959) and consists of a titled, saucer-shaped basin in the south, the Khorat Basin, and a smaller basin to the north, the Sakon Nakhon Basin, separated by the Phu Phan mountain range and drained by the Chi and Mun River systems (Montreal, 1996). The area of study is located in the northern Khorat Basin north of the Chi River (Figure 1).

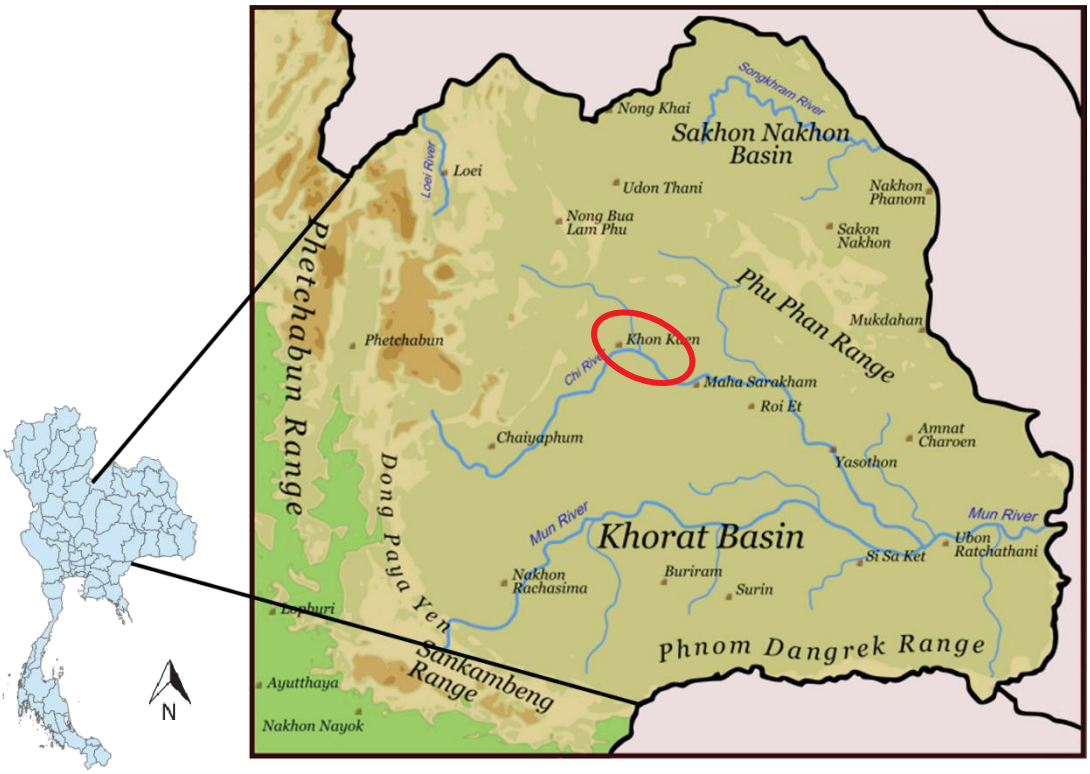

Figure 1: Khorat Plateau indicating locations of the Khorat and Sakhon Nakhon Basins and study location (red circle). (Modified from Damm, H., 2008)

2.3 Geology of the Study Area

The geology underlying the Khorat Plateau consists of eight units of sedimentary bedrock overlain by Quaternary, unconsolidated, terrace and alluvial sediments (Figure 2). The sedimentary rock units range in age from Jurassic to Tertiary in age. The oldest of the sedimentary rock units, the Jurassic Phu Kradung Formation, consists of siltstone, mudstone, and sandstone and is found in the northeast region of the Khorat Plateau. The Phra Wihan Formation, Jurassic-Cretaceous in age, overlies the Phu Kradung and is composed of sandstone, conglomerate, siltstone, and quartzite. There are four Cretaceous units in the area: the Sao Khua Formation, the Phu Phan Formation, the Khok Kruat Formation, and the Maha Sarakham Formation. The Sao Khua Formation is composed of siltstone alternating with sandstone and conglomerate and has been mapped in the northeastern portion of the region. The Phu Phan Formation, mapped in the northern region, comprises a mixture of conglomerate and sandstone. The Khok Kruat Formation is mainly sandstone, siltstone, and shale interbedded with thin beds of gypsum and anhydride and has been mapped in a large region of the Khorat Plateau in the northern and eastern sections. The Maha Sarakham Formation is found locally at many locations. It contains many beds of rock salt interbedded with clastic layers. This formation is the main unit causing salt contamination is the groundwater in parts of the region. The final sedimentary rock formation, Phu Thok Formation, is Cretaceous-Tertiary in age and is divided into three units. The first has been mapped in the central part of the region and consists of mudstone and claystone alternating with siltstone. The second unit, also mapped in the central region, consists of siltstone alternating with sandstone. The third

unit has been mapped in small areas in the southwestern regions consists of sandstone beds (Thana Thoranee Co. Ltd., 2013).

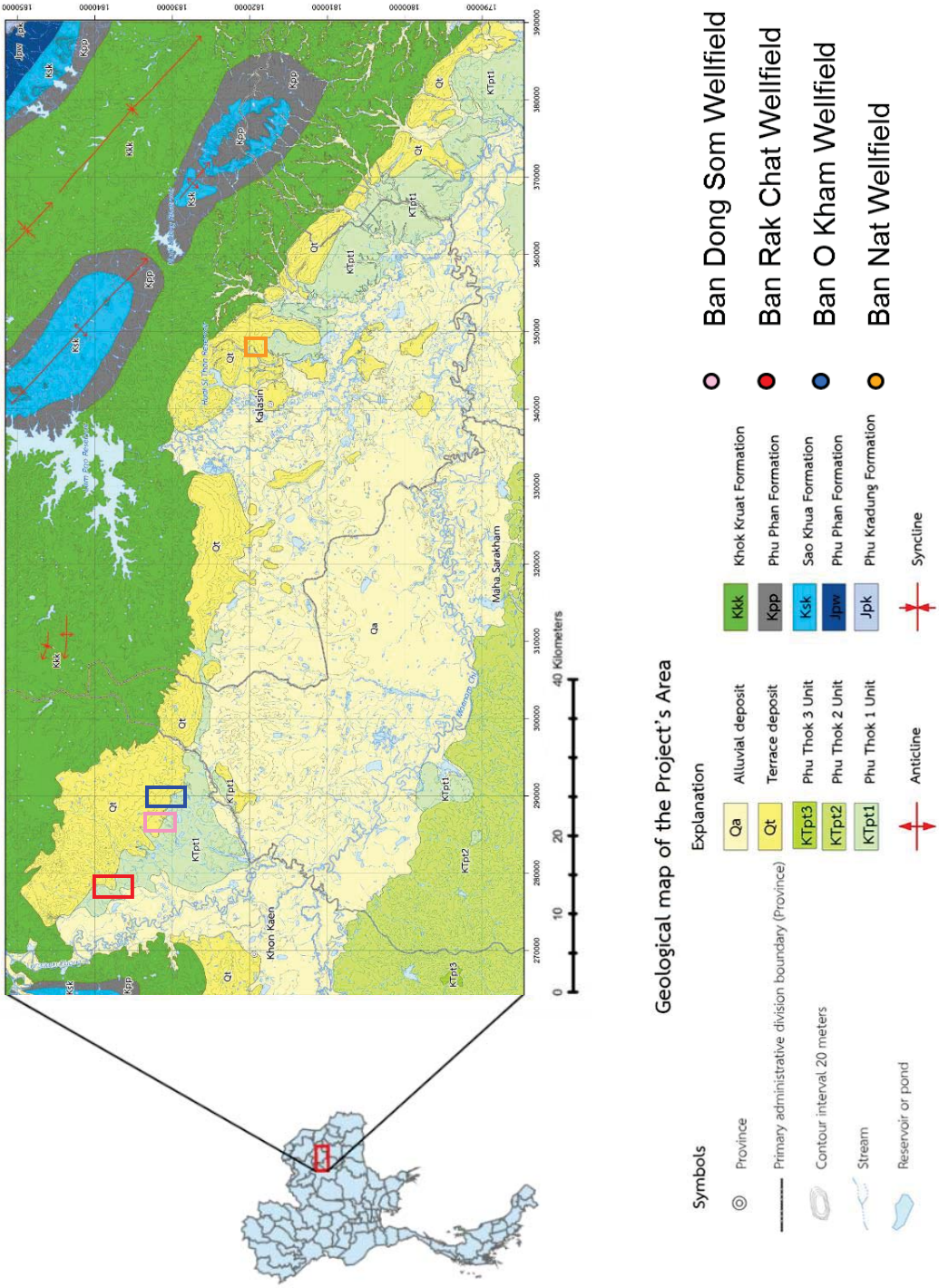

Figure 2: Geologic map and wells evaluated in the study area on the Northern Khorat Basin. Geologic map created by the Thailand Department of Groundwater Resources (modified after Thana Thoranee, 2012).

This study focused on the Quaternary, alluvial and colluvial, terrace deposits comprised of chert, charcoal, petrified wood, tektites, and quartz sediments that were deposited by the ancient Chi and Mun Rivers and erosion of the Phu Phan Mountain Range, Figure 2 (Schulmeister et al., 2015). These sand and gravel deposits form a wedge that support an aquifer system comprised of confined and unconfined aquifers separated by a clay lens. They are directly underlain by the Phu Thok Formation to the southwest and the Khok Kruat Formation to the northeast (Thana Thoranee Co Ltd, 2013). These deposits trend NW-SE and consist of gravel, sand, silt, and rock fragments overlain by lateritic soils (Figure 3). These sediments range in depth from approximately 20 m near the recharge area to over 100 m in the deepest parts (Thana Thoranee Co Ltd, 2013). The sediments are divided into two separate sections, an uppermost, reddish sand and gravel depths of 10-60 m and a lower, dark brown to dark gray sand a gravel at a depth of 30-140 m (Thana Thoranee Co Ltd., 2013). Coarse sediments are generally well rounded and well sorted. Petrified wood, charcoal, quartz, and tektites are commonly found at the surface in the recharge areas and have been noted in driller's logs throughout the unconsolidated sediment (Thana Thoranee Co Ltd, 2013).

Figure 3: Iron-rich, lateritic soils overlie the terrace deposits. Photo near the projects recharge area, northeast of the city of Khon Kaen.

2.3.1 The Australasian Strewn Field

The Australasian Strewn Field, a region containing remnants of a meteoritic impact, is a region covering Australia and Southeast Asia and stretches to the southeastern corner of Africa in which meteoritic tektites are common. These tektites are the result of an impact that occurred around 800,000 years ago in which the location of impact in unknown, though believed to be located in Southeast Asia (Haines et al, 2003). This strewn field is the largest found on Earth and believed to be the result of the largest impact in the past 10 million years. Tektites were formed as the impact melted the terrestrial rocks and caused them to eject a distance away. Tektites are typically composed of approximately 70% SiO_2 (Ridd, et al., 2011). These natural glasses are amorphous silica materials, lacking an internal molecular structure, and are a possible source for the elevated dissolved silica concentrations observed in the aquifer system.

2.3.2 Petrified Wood

Petrified wood found in the alluvial and colluvial deposits are believed to be Mesozoic to Cenozoic in age (Yongdong et al, 2005). Petrified wood has been documented in Upper Jurassic to Lower Cretaceous deposits of the Khorat Group on the Khorat Plateau as well as in the unconsolidated, terrace deposits (Yongdong et al., 2005).

The petrified wood of the Khorat Plateau region is thought to have formed when tropical plants in the region died and buried with flood terrace deposits of the ancient Mun River (Saminpanya et al, 2013). Waters supersaturated with dissolved silica came in contact with the plant resulting in the dissolved silica bonding to the cellulose walls of the plant causing the voids and intercellular spaces in the material to fill with solid silica. The silica initially bonds in an unstable, amorphous form, opal A, before it slowly begins

to crystallize to the more stable form of opal, opal-CT. Opal-CT is a form of opal that contains nanocrystals, crystals less than a nanometer in size. This form of silica will slowly transition to the chalcedony from which will then transition to the most stable from, crystalline quartz (Saminpanya et al, 2013).

2.4 Regional Hydrogeologic and Groundwater Quality Conditions

The terrace deposits are recharged by annual precipitation through the highly permeable laterite soils and generally contains good quality water. The unconfined aquifer is in sand and silt sediment with groundwater expected at 10-40 m. The confined aquifer, containing all developed wells at the areas of study, consists of sand and gravel sediments and yields water of good quality. The deepest parts of the alluvial system contains flowing artesian conditions in which hydraulic heads may reach up to 8 m above land surface (Thana Thoranee Co. Ltd., 2013).

Underlying the system to the northeast lies an aquifer in the consolidated Khok Kruat Sandstone Formation. The Khok Kruat generally contains groundwater of good quality from depths of 20-60 meters with a permeability coefficient of 0.04-2 m/day (Thana Thoranee Co. Ltd., 2013).

The Phu Thok Sandstone Formation underlies the alluvial system to the southwest. The water contained in this formation is trapped within bedding planes and fractures in the sedimentary unit. Flowing artesian conditions are also found in the deepest wells of this formation (Thana Thoranee Co. Ltd., 2013).

2.4.1 Hydrogeology of the Ban O Kham Area

The unconsolidated alluvial and terrace sediments contain a series of confined and unconfined aquifers separated by a clay lens (Thana Thoranee Co. Ltd., 2013). The

groundwater of Ban O Kham (Figure 9) moves from northeast to southwest with hydraulic conductivity (K) values ranging from 0.39-3.92 m/day, storativity values ranging from 7.04 x 10^{-4} to 2.56 x 10^{-2}, and transmissivity values ranging from 4.69 to 46.94 m^2/day (Thana Thoranee Co. Ltd., 2013). In this study, the wells at this location were classified as up-gradient, mid-gradient, and downgradient depending on their location along the flow path (Figure 4). The deepest parts of the aquifer are the most productive locations in the system and produce artesian conditions in which wells may flow up to 8 m above ground surface (Thana Thoranee Co. Ltd., 2013). Precipitation directly recharges the groundwater system through the permeable soils and the water table can fluctuate up to 2 m in response to heavy rainfall (Wongsawat et al., 1992).

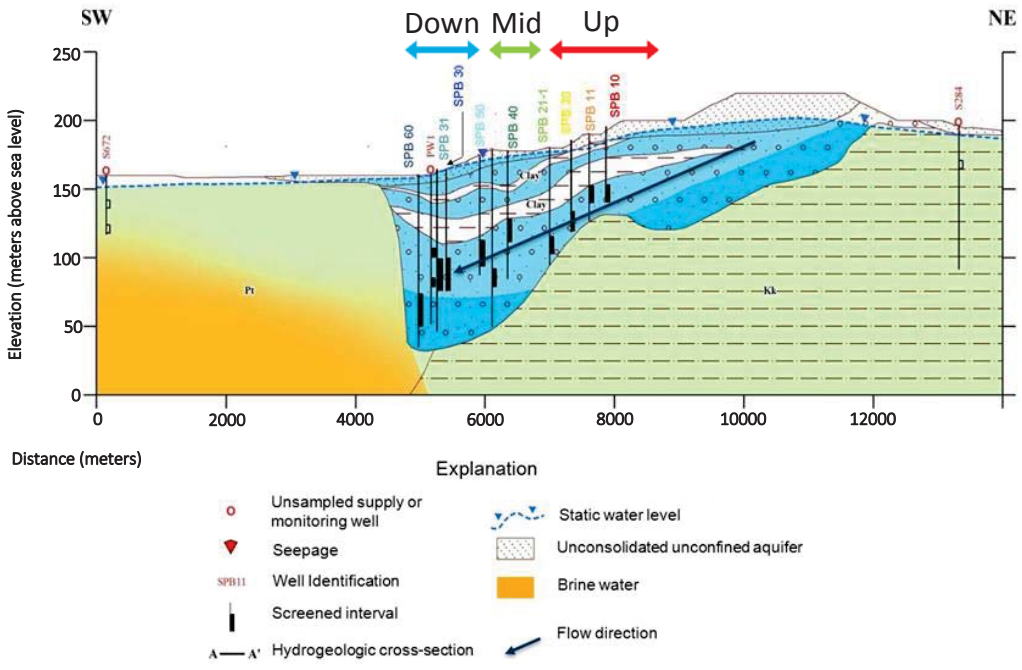

Figure 4: Hydrogeology and monitoring wells at the Ban O Kham site. The highest groundwater yields are located in the deepest parts shown as dark blue. Upgradient wells, labelled in red, are closer to the recharge area to the northeast of the site. Downgradient wells, labelled in blue, are further from the recharge site and near the end of the flow path (Thana Thoranee, Co. Ltd., 2013; modified by Schulmeister et al., 2015)

2.5 Climatic Setting of Northeastern Thailand

The climate of Northeastern Thailand is classified in the Köppen climate classification as Tropical Savannah (Pidwirny et al, 2006). Tropical climates are recognized by temperatures in every month averaging over 18°C. Savannah climates have distinct dry and rainy seasons with the dry season occurring from November to April and the rainy season occurring from May to October (Pidwirny et al, 2006). The average annual rainfall of Northeastern Thailand is approximately 1400 mm per year, with over 80% falling in the rainy season. The average temperature for the region is 26.8°C, the warmest month being April (29.7°C) and the coolest being December (22.9°C; Royal Meteorological Department, 2015).

Drought conditions in Northeastern Thailand increase the evaporation of surface water resources and impact the storage of water in surface and subsurface reservoirs (Jayakumar and Lee, 2017). Recent droughts in the region are lowering dam volumes by up to 10% causing the relocation of water from the Mekong River (Fox, 2016). The drought is likely due to the El Niño phenomenon, occurring every two to seven years, which is a series of climatic changes resulting in drought in many areas of the world (National Drought Mitigation Center, 2017). Conditions prior to and during the 2011-2012 sampling periods included wetter than usual conditions followed by four years of below average rainfall during the 2016 sampling period (Figure 5; World Weather Online, 2017). Monsoon conditions during the rainy season vary annually.

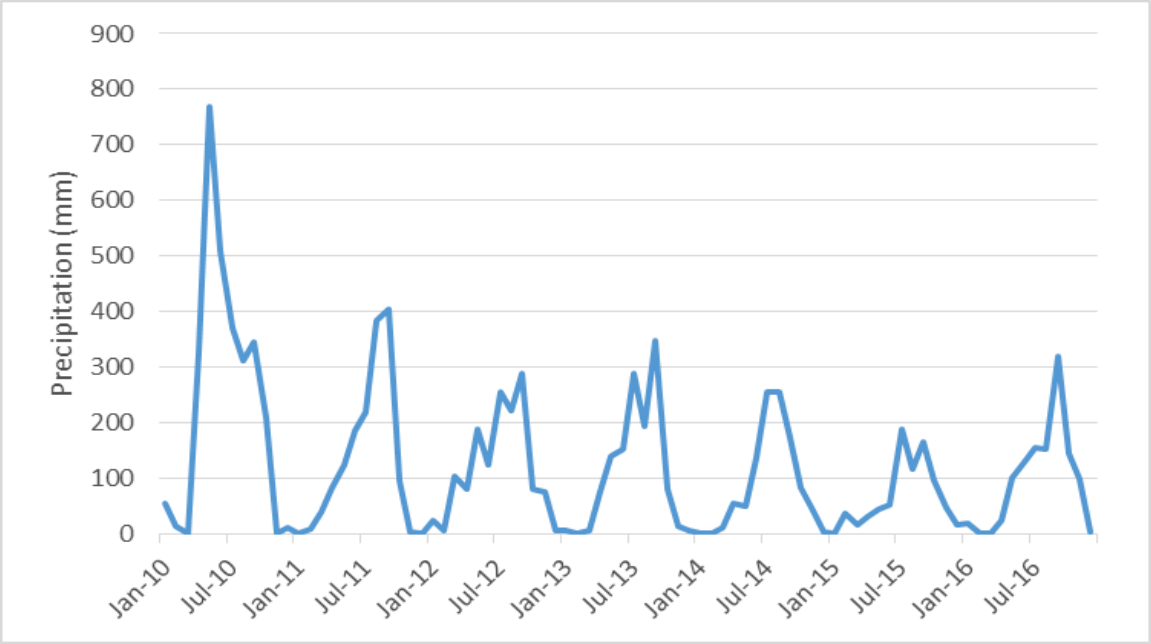

Figure 5: Rainfall at a Khon Kaen stations from 2010 to 2016 (World Weather Online, 2017).

2.6 Previous Research

Previous research was conducted to determine the quality and quantity of the groundwater of the Khorat Plateau for domestic and agricultural use. The following sections describe three water resources surveys conducted by the United States Geological Survey, the Thailand Department of Groundwater Resources, and Emporia State University and Khon Kaen University.

2.6.1 Ground Water Exploration Project

In the mid 1950's, water shortages during the dry seasons of each year in Northeastern Thailand led the United States Geological Survey's Ground Water Exploration Project, consisting of the Report on Ground Water Exploration and Development of the Khorat Plateau Region (Haworth et al, 1959) and the Ground Water Resources Development of Northeastern Thailand (Haworth, 1966). This project,

financed under the joint Thai Government-United States Government Operations Mission, resulted in the drilling of 1862 exploration wells in the attempt to obtain the information on groundwater chemistry, information about the subsurface strata, and hydrogeologic field parameters for the planning and development of water resources for the 7.8 million residents of the region. Results indicate extremely high silica concentrations, 200 mg/L SiO_2, and pH values as low as 4.2 in some locations in the bedrock aquifers (Haworth et al., 1959). Elevated silica concentrations lead to the interest in groundwater silica of the region.

The USGS Ground Water Exploration Project began with a preliminary study in late 1954 outlining areas containing ground water of good quality and quantity in order to determine the location of wells to be developed. The USGS collected data from 158 pre-existing representative wells and springs and described geological exposures at the Khorat Plateau (LaMoreaux et al., 1958). A total of 1011 exploration wells were drilled between November 1955 and December 1963 in 22 Changwats (provinces) on the Khorat Plateau. Of the 1011 drilled wells, 795 were utilized as production wells, containing water of good quality or slightly brackish water to be used for limited purposes, and 216 were abandoned due to high salinity, dryness, or mechanical difficulties. The production wells containing good quality water yielded between 2 and 1020 gallons per minute with depths in the range of 7 to over 600 m (Haworth et al., 1966).

Characteristics of the underlying bedrock formations were determined using geophysical analysis, aquifer tests, and chemical analysis. Electric logging was used on several boreholes to determine the identity and thicknesses of underlying strata using spontaneous potential (SP) and resistivity readings. Results were utilized to correlate the

strata between wells and to determine where salt formations may contaminate the ground water system. Pump tests were performed at several locations to determine storativity and transmissivity. Storativity coefficient values ranged from 7.3×10^{-4} to 3.96×10^{-3} and transmissivity coefficient values ranged from 15000 to 68000 gpd per ft. Analysis for major ions, dissolved silica, heavy metals, nutrients, hydrogen, fluoride, carbon dioxide, chloride, manganese, carbon, TDS, pH, EC and TSS was completed for 738 production wells indicated water types of different areas on the Khorat Plateau using major ion analysis. Waters of alluvial and terrace deposits were generally Ca^{2+}-SO_4^{2-} type waters while the waters of the Khorat Basin and Sakon Nakhon Basin were predominately Ca^{2+}-HCO_3^- type. Unusually high silica concentrations of up to 200 mg/L SiO_2 were present in some areas of the region (Haworth et al., 1966). The results of these assessments were utilized to determine the groundwater availability of the Khorat Plateau, shown in Figure 6, as well as the groundwater quality.

Results of the Ground Water Exploration Project demonstrated sufficient ground water availability throughout nearly all of the Khorat Plateau. Due to the extensive coverage of the drilling, high potential areas were located that yield water of good quality to be used for domestic, agricultural, and industrial purposes. Groundwater of all localities was deemed usable for livestock consumption. Most groundwater can be used for domestic uses with a few exceptions in locations where water hardness is too high and where sulfate and chloride concentrations are high. For agricultural purposes, groundwater from shale and siltstone bedrock aquifers is not satisfactory due to low yields. Alluvial aquifers and sandstone and limestone bedrock aquifers, however, may provide a good source though they had yet to be used for these purposes. Depending on

the industry, the waters may or may not be used for industrial purposes. The high NaCl content present in some locations may cause corrosion and the high silica, iron, and calcium concentration may cause precipitation on boilers (Haworth et al, 1966).

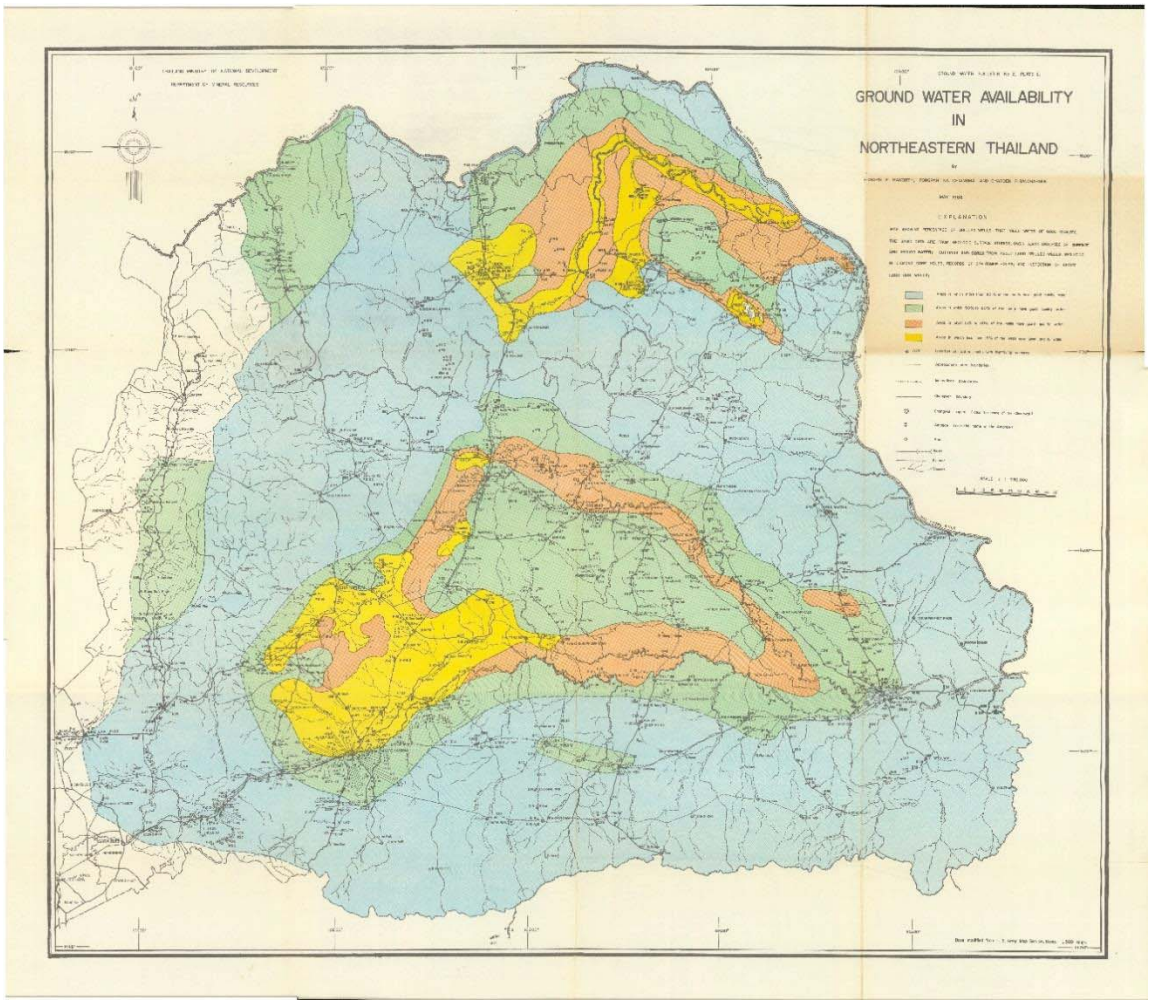

Figure 6: Locations of available groundwater on the Khorat Plateau (Haworth, 1966).

2.6.2 The Sustainable Development of Flowing Artesian Wellfield in the Central Chi River Basin Project

In 2012, groundwater in the Khorat Plateau was assessed by the Thailand Department of Groundwater Resources (DGR) under King Bhumibhol Adulyadej's order to protect and preserve Thailand's water resources. The Sustainable Development of Flowing Artesian Wellfield in the Central Chi River Basin Project aimed to study unconsolidated-confined aquifers in the region, set the groundwater observation network for monitoring, construct groundwater models for sustainable management, to design and establish pilot systems on groundwater springs for consumption and agriculture purposes, and to design suitable recharge systems for maintaining of groundwater resources in order to have sufficient water resources during drought seasons. The Sustainable Development of Flowing Artesian Wellfield in the Central Chi River Basin Project was carried out by Thana Thoranee Company Limited and focused on the unconsolidated, confined aquifers within the projects 8,500 km^2 covering parts of the provinces Khon Kaen, Maha Sarakham, Kalasin, and Roi Et (Thana Thoranee Co. Ltd., 2013). The data obtained during this research was further evaluated in this research.

A hydrogeologic study was conducted in which wells were inventoried, soil and rock were analyzed for infiltration rates, geophysical surveys were done, topography of the land was surveyed, land and water were studied for utilization purpose, and exploration drilling was completed for sediment core and grainsize analysis to select three study locations, the Ban Rak Chat, Ban O Kham, and Ban Nat areas, as high-potential areas for groundwater spring. The aquifers of the three study areas were compared and analyzed using pumping tests to determine, water levels, permeability,

transmissivity, storativity, and hydraulic conductivity and safe yields. The hydraulic conductivity ranged from 0.28 to 3.61 m/day, storativity coefficient values ranged from 2.10×10^{-4} to 3.15×10^{-2}, and transmissivity ranged from 4.62 to 57.89 m^2/day. Using this data, the Ban O Kham site was found to have the highest potential for groundwater spring (Thana Throanee Co. Ltd., 2013).

The three sample areas contain twenty-five monitoring wells, seven at Ban Rak Chat, eleven at Ban O Kham, and seven at Ban Nat, which were sampled six times between October 2011 and August 2012 for laboratory analysis and are presented as Appendix A. The chemical quality of the groundwater samples was analyzed in the laboratory for major ions, iron, manganese, copper, silica, alkalinity, nitrate, fluoride, boron, phosphate, and arsenic. Data from this investigation can be viewed in Appendix A. Other parameters, such as pH, hardness, total dissolved solids (TDS), turbidity, color, and electrical conductivity, were also measured (Thana Thoranee Co. Ltd., 2013).

The final phase of the DGR project consisted of the establishment of the water collection and distribution system. This involved the installation of additional production wells in the Ban O Kham area and of automatic water-level recorders in each of the study locations. The production wells were put into place for pumping and sampling purposes and concluded that the major aquifer consists of course to very course grained sand and gravel. Three automatic water level recorders, in each a recharge well, a development well, and a discharge well, were placed at each of the study sites. A system was designed for water collection and distribution at Ban O Kham which utilized the production wells as well as two observation wells. These wells were connected to water tanks and PVC pipes for distribution of the water resources (Thana Thoranee Co. Ltd., 2013).

The Sustainable Development of Flowing Artesian Wellfield in the Central Chi River Basin Project was successful as high potential spring areas were determined allowing for available water resources during drought season without the consumption of energy.

2.6.3 Emporia State University and Khon Kaen University Evaluation of Hydrogeochemistry of the Flowing Artesian Wellfield of the Khorat Plateau, Northeastern Thailand

Groundwater chemistry reported by the DGR in 2012 were evaluated by an Emporia State and Khon Kaen team of scientists (Schulmeister et al., 2015). This research focused on the Ban O Kham study area from the DGR study. The Ban O Kham area covers over 900,000 m^2 and is located between the Chi and Phong Rivers. It lies on Cretaceous to Tertiary sedimentary rocks overlain by Quaternary unconsolidated sediments (Thana Thoranee Co. Ltd., 2013). The primary bedrock aquifers lie in the Phu Thok Formation, Cretaceous and Tertiary sandstone, claystone, and siltstone, and in the Khok Kurat Formation, Cretaceous sandstone and siltstone. The groundwater of these bedrock formations is generally of good quality though lower portions of the units yield brackish waters due to rock salt present in the Mahasarakham Formation, present between the two bedrock formations at various locations (Schulmeister et al., 2015).

Chemical analysis for nine observation wells were collected on a bi-monthly schedule during 2011-2012 by the Thailand Department of Groundwater Resources and were used in the investigation by Schulmeister (2015) and also in this study. They included major ions, silica, iron, and manganese concentrations were recorded and TDS, EC, pH, and turbidity (Thana Thoranee Co. Ltd., 2013). An analysis of major ions

concluded that there was a change in water chemistry from Ca-Mg-Cl-SO_4 to Ca-Mg-HCO_3 water type down the flow gradient. Iron and manganese analysis suggested the presence of reducing conditions promoting the existence of dissolved iron and manganese. A comparison of pH to dissolved silica concentrations concluded an increase of dissolved silica, along with a decrease of pH, down the flow gradient suggesting the chemical weathering of silicate minerals as water infiltrates highly weathered soil (Schulmeister et al, 2015). This work is the basis for this thesis.

2.7 Locations used in this Study

This research evaluated data reported by the DGR during 2011-2012 as well as samples obtained in the summer of 2016. In 2011-2012, Ban O Kham, Ban Rak Chat, and Ban Nat were sampled by the DGR while in 2016, Ban O Kham and Ban Dong Sam were visited by Emporia State University and Khon Kaen University geologists. Several wells from Ban Swang and Ban Haeo were analyzed during the 2016 sampling period. Although data from these wells are included in the thesis, well construction details are not available, prohibiting a thorough analysis of the results. This research focuses mainly on the data obtained from the Ban O Kham study location due to the extensive amount of information that has been obtained from this site.

2.7.1 The Ban O Kham Study Area

Ban O Kham is a village in the Khon Kaen Province that lies 16 kilometers northeast of the city of Khon Kaen. Eleven wells were sampled at this study location by the DGR and nine were visited during the summer of 2016, Figure 7. The study area covers a total of 0.9 km^2 and is in the range of 158-170 meters above sea level. It is covered by agricultural fields of cassava, rice, and eucalyptus (Thana Thoranee Co. Ltd.,

2013). Groundwater flows quicker in locations near the upgradient wells as indicated by the equipotential lines in Figure 8. Flowing artesian wells are present in the deepest parts of the aquifer in wells SPB30, SPB31, SPB50, SPB60, and SPB 40.

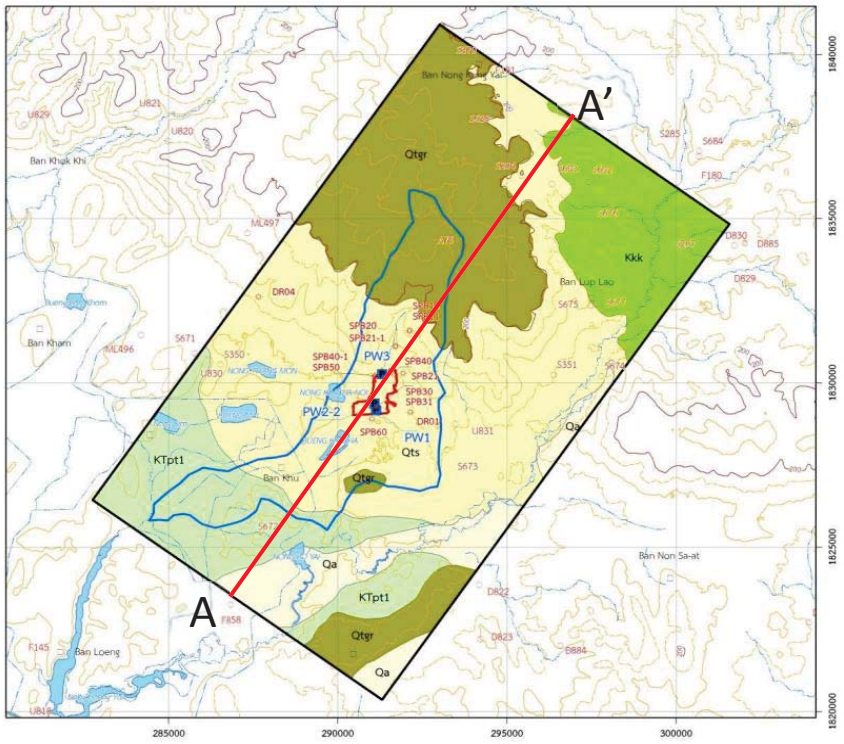

Figure 7: Well locations and line indicating cross section at Ban O Kham. Modified after Thana Thoranee Co. Ltd., 2013

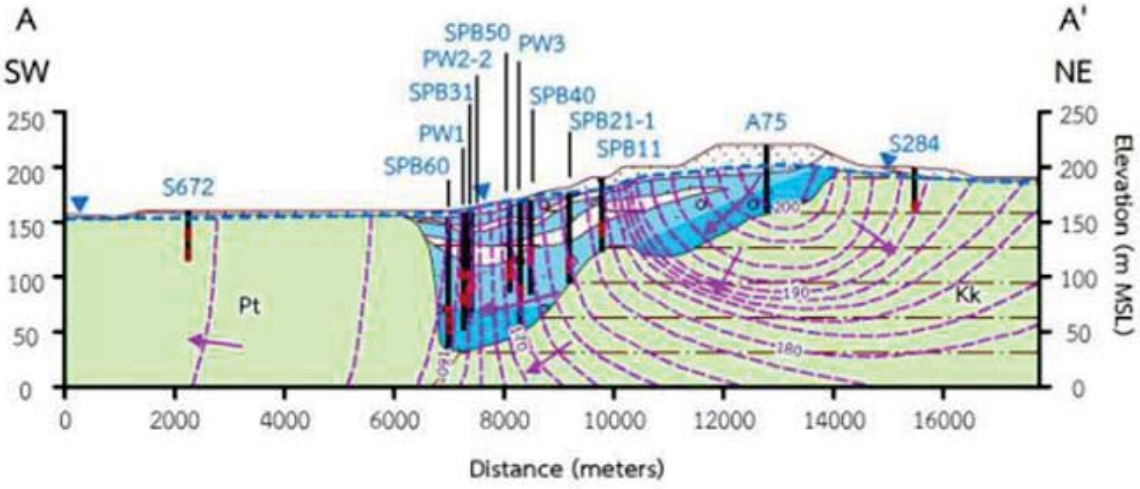

Figure 8: Groundwater flow and sampled wells of the Ban O Kham well site. Production wells (PW) were installed after the 2012 sampling periods (Thana Thoranee Co. Ltd., 2013).

2.7.2 The Ban Rak Chat Study Area

Ban Rak Chat is a village 23 kilometers north of the city of Khon Kaen in the Khon Kaen province. The wellsite contains seven wells that were visited by the Thailand DGR in 2011-2012, Figure 9. The study site, comprising an area of 0.8 km^2, is covered in fields of rice, grove, eucalyptus, rubber tree, cassava, and sugar cane. It is 172-178 meters above sea level (Thana Thoranee Co. Ltd., 2013). The cross section image suggests the groundwater slows in downgradient wells as indicated by equipotential lines, Figure 10. Flowing artesian wells are present in the deepest parts of the aquifer in wells SPA30, SPA21 and SPA40.

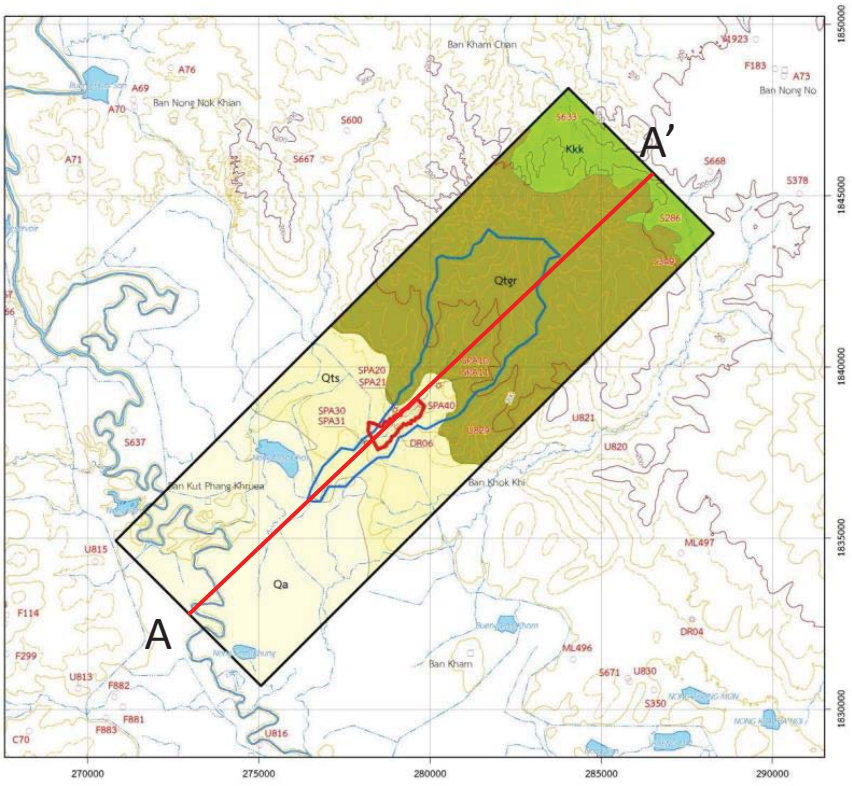

Figure 9: Well locations and cross section line at the Ban Rak Chat study site. Modified after Thana Thoranee Co. Ltd., 2013

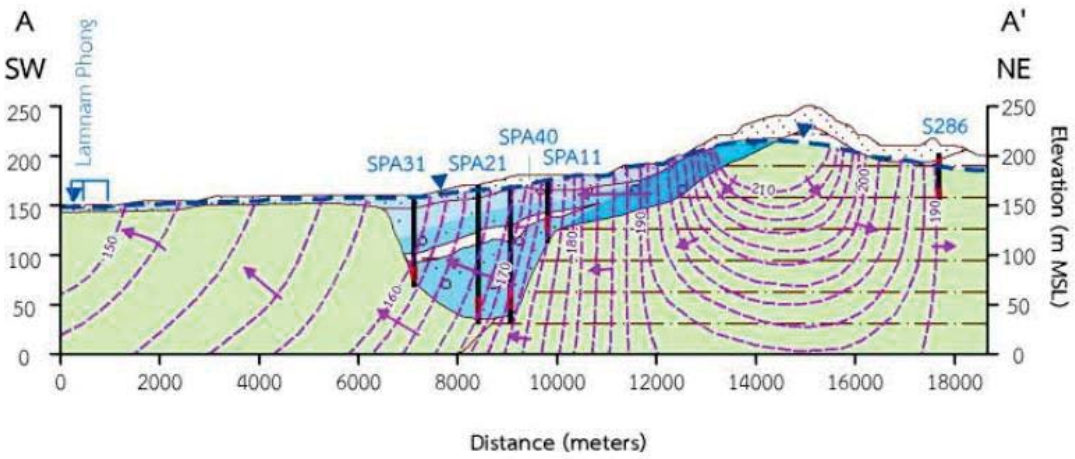

Figure 10: Cross Section of A-A' at the Ban Rak Chat location (Thana Thoranee Co. Ltd., 2013).

2.7.3 The Ban Nat Study Area

Ban Nat is a village approximately 23 kilometers southeast of the city of Roi Et in Roi Et province. The wellsite, Figure 11, contains seven wells that were visited by the Thailand DGR in 2011-2012. The area is mainly covered by cassava fields with some rice, eucalyptus, rubber tree, grove, and mango fields. Its elevation is in the range of 150-160 meters above sea level (Thana Thoranee Co. Ltd., 2013). Unlike the other two locations, equipotential lines indicate groundwater moves faster in mid and downgradient wells, Figure 12. Flowing artesian wells are present in the deepest parts of the aquifer in wells SPC20, SPC21, SPC30, and SPC31.

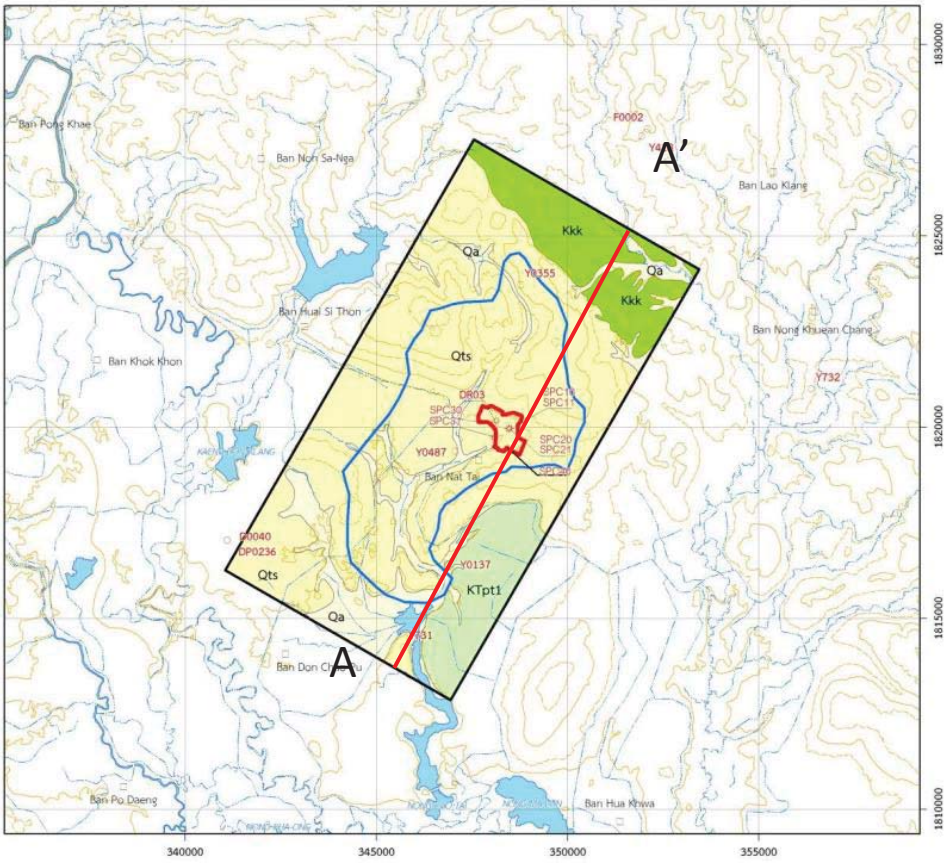

Figure 11: Well locations and cross section line at the Ban Nat study site. Modified after Thana Thoranee Co. Ltd., 2013

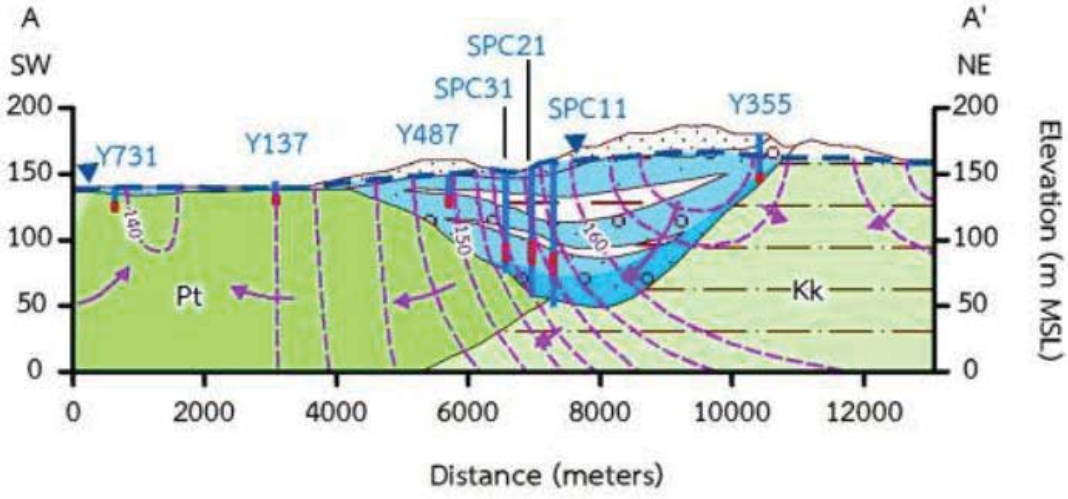

Figure 12: Hydrogeology of the Ban Nat study site (Thana Thoranee Co. Ltd., 213).

2.7.4 The Ban Dong Sam Study Area

Ban Dong Sam, located about 24 kilometers northeast of the city of Khon Kaen, is a village in the Kranuan district, Khon Kaen province. A total of seven wells were visited near the village (Figure 13). The Ban Dong Sam wellsite was also investigated by Dr. Marcia Schulmeister in 2015 and Dr. Rungruang Lertsirivorakul in 2010. The village is surrounded by agricultural fields of rice patty, cassava, and sugar cane.

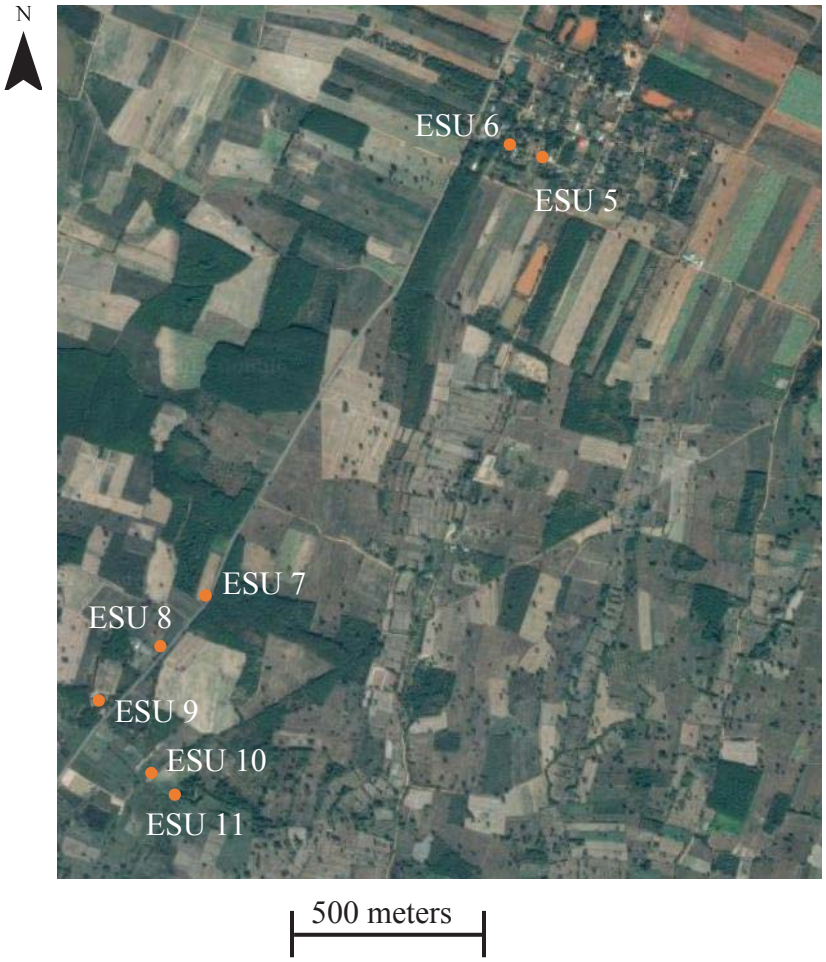

Figure 13: Well locations, indicated as orange dots, at the Ban Dong Sam wellsite. The city of Ban Dong Sam can be seen in the top right corner of the map surrounded by agricultural fields. Aerial image derived from Google Maps.

CHAPTER 3: METHODS

3.1 2016 Sample Collection

During the summer of 2016, wells from the Ban O Kham and Ban Dong Sam areas were resampled as part of this study. Sample locations from these two locations are seen in Figure 14. Groundwater samples were collected along the groundwater flow path at up, mid, and downgradient wells at the Ban O Kham study site and along a proposed recharge path and at locations near the expected recharge and discharge at Ban Dong Sam site, Figure 13. Water levels were measured using an electric measuring tape. Wells with standing water were purged to achieve a representative sample using dedicated pumps. At flowing wells, 1.5 L of groundwater were collected directly at the well head. Approximately 500 mL of each sample was acidified with 5 mL of 15.8 M nitric acid to acidify the samples to a pH of approximately 2. All samples were chilled at 4° C until laboratory analysis. At most sample locations, a calibrated Troll 9500 Multiparameter Sonde measured temperature, pH, ORP, dissolved oxygen concentration, and electrical conductivity, utilizing a flow through cell on flowing wells, until the parameters stabilized (In Situ, 2009). Calibration was completed prior to the sampling and again after the sampling was complete. The calibration parameters for the multiparameter sonde are presented in Appendix B. Additional handheld pH and electrical conductivity probes were also used on site to provide verification of the methods by Khon Kaen University Geotechnology graduate students.

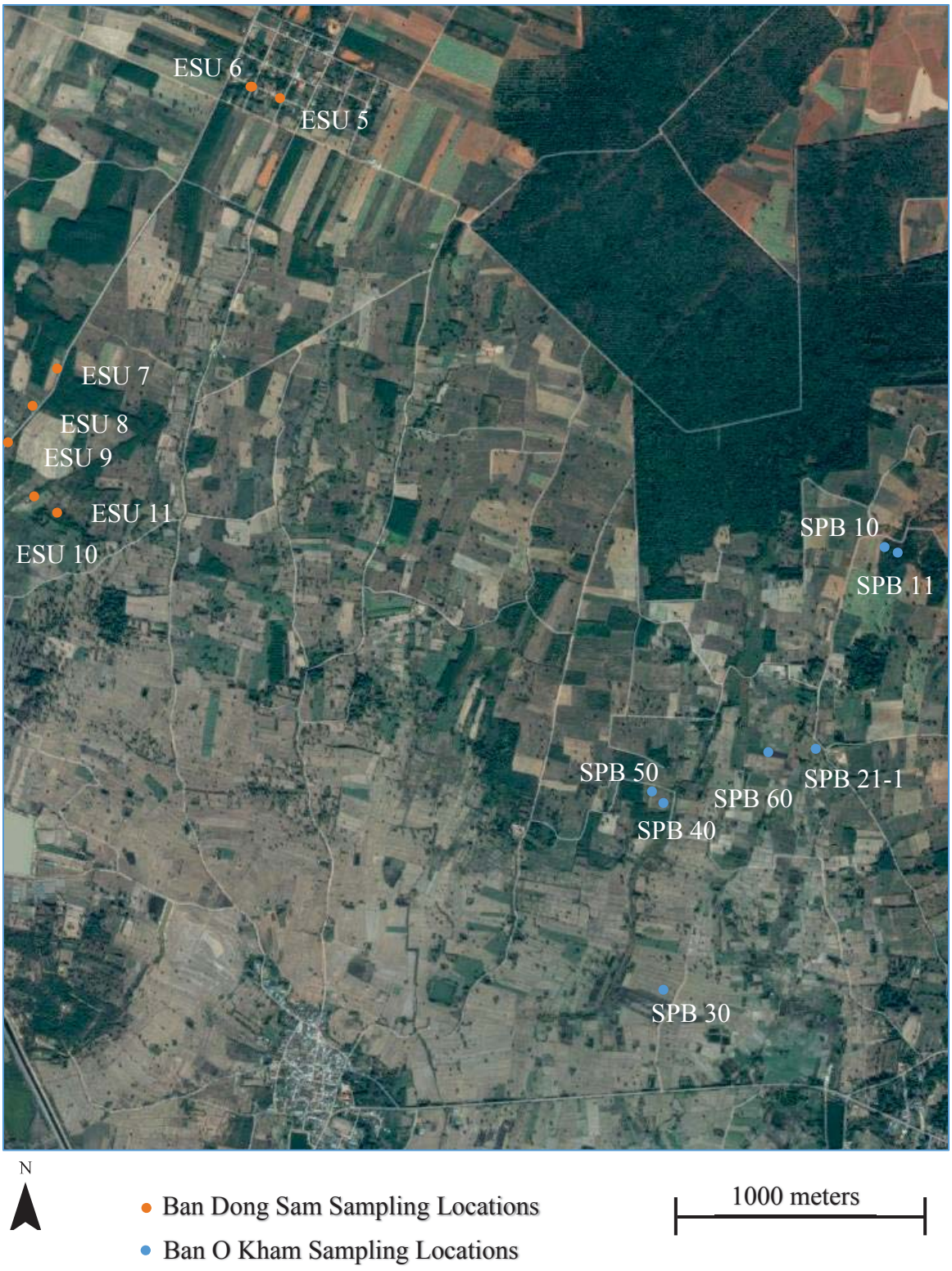

Figure 14: Sampling locations for the 2016 sampling period.

3.2 Major Ion Analysis

Major ion concentrations were measured at the Department of Geotechnology at Khon Kaen University flame atomic absorption spectroscopy. Calibration standards were made from stock solutions for each ion. Acidified samples were analyzed three times using the atomic absorption instrument. Procedures and calibration results are presented in Appendix D.

3.3 Alkalinity Analysis

Samples were analyzed in the Khon Kaen Unversity water chemistry laboratory for alkalinity by titration using a Methyl Orange indicator and 0.02 N Sulfuric Acid (H_2SO_4), (EPA, 1974). The sulfuric acid was made by diluting 11 mL of 1.8175 N H_2SO_4 solution to 1L of deionized water. The acid was standardized by titration against a 0.05 N Sodium Carbonate (Na_2CO_3) solution. The indicator has a color change at pH 4.4 from yellow to orange. 100 mL of each sample was measured into a 250 mL beaker at room temperature. Four drops of Methyl Orange were added to each sample and the solution was placed on a magnetic stir plate. The solution was titrated with the 0.02 N H_2SO_4 until the solution turned a light orange color. To assure the method produced accurate results, three of the samples were titrated using a pH meter (APHA, 1998). All samples were not analyzed using this method due to lack of time with the necessary laboratory equipment. Samples from ESU1, ESU2/SPB60 and ESU4 were titrated using the pH meter. Titration results are presented in Appendix A.

3.4 Dissolved Silica Analysis

Dissolved silica concentrations were determined using the Silicomolybdate Spectrophotometric method outlined in Appendix E. Prior to analysis, samples were

filtered with 0.45-micron Whatman filter papers and a vacuum filtering system. During the analysis, samples from ESU2, ESU6, ESU7, ESU8, ESU9, and ESU10, developed an iron oxide precipitate after sitting overnight. Before filtration, these samples were placed in a centrifuge for 15 minutes to remove the iron oxide and color that developed from the precipitate. Standards were made using a 1000 mg/L SiO_2 stock solution. 100 mL standards were created with the concentrations of 0.1 mg/L, 1 mg/L, 10 mg/L, 20 mg/L, 30 mg/L, and 40 mg/L to produce a calibration curve.

The standards and samples were analyzed for silica concentration using a Lambda 2 spectrophotometer (Morris, S., 1989) and Hach method #8185 (Hach, 2005). The method utilized pre-measured reagents to produce a yellow color to analyze at wavelength 390 nm. Wavelength determination was determined using the method in Appendix E. A molybdate powder pillow is dissolved into 10 mL of sample. An acid powder pillow is dissolved in solution and a 10-minute reaction period is enforced. The molybdate reacts with silica and phosphate in the solution forming complexes in acidic environments, forming a yellow color. A citric acid powder pillow is then dissolved in solution and a two-minute reaction period is allowed. The citric acid will remove phosphate complexes, leaving only the silica molybdate complexes (Hach, 2005). Deionized water is placed in a 1 cm cuvette to zero the spectrophotometer. Sample solutions are placed into a 1 cm cuvette and analyzed in the spectrophotometer. Absorbance values were read three times for each sample. Silica concentrations are displayed in Table 1.

3.5 Total Dissolved Solids

Total dissolved solids (TDS) concentrations were analyzed in the laboratory utilizing an evaporating dish (American Public Health Association, 1998). An evaporating dish evaporates solvents from solution, leaving behind only the dissolved substances. The dish is heated to 180°C for 24 hours in an oven and weighed before 25 mL of filtered groundwater sample is added. The sample is placed in the oven at 180°C for 24 hours to allow the solvent to evaporate. The solution is removed from the oven and immediately weighed. To determine TDS concentrations (mg/L), the following equation is used:

$$\boldsymbol{TDS}\left(\frac{\boldsymbol{mg}}{\boldsymbol{L}}\right) = \frac{(\boldsymbol{A}-\boldsymbol{B})\times\mathbf{1000}}{\boldsymbol{sample\ volume}}$$

A- Weight of dried dissolved residue in dish (g)

B- Weight of empty dish (g)

3.6 Data Validation

Data validation analysis was completed on major ions to evaluate the integrity of the analysis. A charge balance, a TDS comparison, and an EC-TDS comparison was completed on the chemical results. Validation data can be observed in Appendix F. Due to a problem with 1 sample, ESU 1, it could not be analyzed for anions and could not be validated.

3.6.1 Charge Balance

A cation-anion charge balance is completed on each sample to determine if the samples are electrically neutral. The sum of all the cations, in milliequivalents per liter (meq/L), is compared to all the anions (meq/L) in solution to determine the difference.

An acceptable difference in water analysis for data in which the anion sum is less than or equal to 3 meq/L is ±0.2 meq/L. When the anion sum is in the rand of 3.0 and 10.0 meq/L, the percent difference must be determined. The acceptable percent difference is ± 2% (American Public Health Association, 1998). The percent difference is calculated using the following equation:

$$\boldsymbol{Percent\ Difference} = \mathbf{100} * \frac{\boldsymbol{\Sigma\ Cations} - \boldsymbol{\Sigma\ Anions}}{\boldsymbol{\Sigma\ Cations} + \boldsymbol{\Sigma\ Anions}}$$

An analysis was done comparing major cations to major anions along with an analysis comparing major cations plus iron to major anions. Due to low TDS values and high iron content in the overlying lateritic soils, iron may be a contributor to the dissolved solids in the system.

3.6.2 Measured vs. Calculated Total Dissolved Solids (TDS)

When comparing measured and calculated TDS, the measured value should be higher than the calculated value because a contributor to the TDS value may not be included in the calculated concentration. Ions (mg/L) are summed to calculate TDS in the following equation:

$$\boldsymbol{TDS} = \boldsymbol{Na} + \boldsymbol{K} + \boldsymbol{Mg} + \boldsymbol{Cl} + \boldsymbol{SO4} + \boldsymbol{SIO3} + \boldsymbol{NO3} + \boldsymbol{F} + \mathbf{0.6}(\boldsymbol{Alkalinity\ as\ CaCO3})$$

When finding the calculated value, dissolved silica as SiO_2 was used in place of SiO_3. The calculated value should be no more than 20% larger than the measured value. The ratio between measured over calculated TDS should fall between 1.0 and 1.2 (American Public Health Association, 1998). Comparisons were made for field and laboratory TDS values.

3.6.3 Comparison of Calculated TDS to Electrical Conductivity

In natural waters, the ratio between calculated total dissolved solids (TDS) and electrical conductivity (EC) is between 0.55 and 0.70. If the value falls below 0.55, the lower ion sum is suspected to be incorrect. If the value is above 0.70, the higher ion sum is suspected. The value may reach as high as 0.80 when poorly dissociated calcium and sulfate ions are present in solution (American Public Health Association, 1998).

3.7 Presentation of Major Ion Chemistry

Piper diagrams were utilized for a visual display of the major ion data. Piper diagrams are a set of diagrams that show the percent composition of major ions in a solution. A trilinear diagram is made for major cations as well as a diagram for major anions. A diamond-shaped diagram between the two diagrams represents the composition of water in which all major ions are included.

The United State Geological Survey's piper diagram program, GW_Chart, was used to develop piper diagrams for the well sites (Winston, 2000). The concentrations of major ions (meq/L) for each wellsite were entered into the software and point was generated on the diagram.

3.8 Determination of Silica Saturation Indices

Saturation indices determine whether the conditions exist for the dissolution or precipitation of a solid in solution. It is a value utilizing the ion activity product (IAP) and solubility product constant (Ksp) in which a positive value indicates the conditions for precipitation and a negative value indicates conditions for dissolution. The Ksp is the amount of analyte in solution at equilibrium while the IAP is the amount of analyte in solution, whether it be in or out of equilibrium (Aqion, 2017). Differences in the

solubility of silica rocks and minerals will result in differences in saturation index values. The following equation demonstrates how these values are calculated.

$$Saturation\ Index\ =\ log_{10}\ (IAP\ /\ Ksp)$$

Saturation indices were calculated using the United States Geological Survey's chemical modelling program PHREEQC (Parkhurst and Appelo, 2013). Field and chemical parameters were entered into an input file. Field parameters utilized are water temperature, pH, and pe. The pe is the reduction potential which measures the tendency of a species to obtain electrons. The pe was calculated using water temperature and ORP in the following equations:

$$\boldsymbol{Eh = ORP(mV) + 197\ mV}$$

$$\boldsymbol{pe = \frac{F}{2.303\ RT} Eh(V)}$$

where F is the Faraday constant (23.1 kcal/V), R is the gas constant (0.00199 kcal/(mol*K) and T is the temperature (K) (Fetter, 2001). All chemical parameters available were utilized in the input file for the chemical model. The program uses the input information to determine saturation indices for rocks and minerals that can exist in the system. The saturation indices for silica rocks and minerals, quartz, chalcedony, and amorphous silica, were recorded for at different wells down the gradient at different sampling dates. These three forms of silica were examined because…

3.8.1 Assumptions made in Interpretation of Data

Due to a lack of field measured parameters in the 2011-2012 sampling periods, values from the summer 2016 research were utilized for modeling purposes. Field data included temperature and ORP. To correct for instrument drift (as discussed in Appendix x), Eh was calculated using the ORP value read from the instrument as well as a 10%

increase of that value. The 10% increase in the ORP value proved to have no impact on the Eh calculation.

CHAPTER 4: RESULTS

4.1 Evaluation of Laboratory Analysis

In 2011-2012, 150 groundwater samples were retrieved from 25 monitoring wells over the period of a year at the Ban O Kham, Ban Rak Chat, and Ban Nat field sites. During the summer of 2016, 17 groundwater samples were taken out of the 19 visited wells in the Ban O Kham and Ban Dong Sam field sites. A quality control evaluation of sample handling and laboratory analyses was conducted to ensure the validity of the data and can be viewed in Appendix F and are summarized in the following sections.

4.1.1 Charge Balance

Analysis of charge/mass balance was completed for each sample. Charge balances for the 2011-2012 samples all met the criteria for acceptable differences confirming the data is valid. The addition of iron to the cations was not necessary when analyzing the charge balance. The 2016 data indicate 8 out of the 16 samples within the acceptable charge balance range. Out of the eight samples, six required the addition of iron to the cations for the ions to balance, Appendix F.

4.1.2 Measured vs. Calculated Total Dissolved Solids (TDS)

Measured and calculated total dissolved solids were compared for 16 samples of 2016 data laboratory and field data. For the calculated TDS vs field data, 11 of the 16 samples had an acceptable ratio between 1.0 and 1.2. For the laboratory TDS analysis, the ratio was acceptable in 10 out of the 16 samples.

4.1.3 Comparison of Calculated TDS to Electrical Conductivity

A comparison of calculated TDS against electrical conductivity was completed on 16 samples of 2016 data. Of the 16 samples, 6 fell into the acceptable ratio range of 0.55-0.70.

4.2 Major Ion Analysis at Four Locations

Calcium, sodium, potassium, magnesium, bicarbonate, chloride, sulfate, dissolved silica, and iron were analyzed in 19 wells in Ban Haeo, Ban O Kham, and Ban Dong Som, Table 1. A wide range of calcium (0.46-78.99 mg/L), sodium (1.51-59.20 mg/L), bicarbonate (9.76-149.45 mg/L), chloride (062-97.72 mg/L), sulfate (0.03-163.02 mg/L), and iron (0.00-109 mg/L) were observed in the system. Potassium concentrations were observed at a range of 0.25-3.26, magnesium concentrations ranged from 0.79-10.44 mg/L, and silica concentrations ranged from 11.73-49.25 mg/L.

Data in Table 1 and Appendix A were used to characterize the waters of Ban Dong Sam, Ban O Kham, Ban Rak Chat, and Ban Nat (Figures 15 A-D). The groundwater of Ban O Kham changes from Ca^{2+}-Cl^{-}—SO_4^{2-} type, upgradient, to Ca^{+2}-Na^{+}-HCO_3^{-} downgradient, with the exception of SPB 21-1. The chemistry of well SPB 21-1 appears to be influenced by the underlying Khok Kruat bedrock formation. The water at Ban Rak Chat is characterized as Ca^{2+}-HCO_3^{-}, upgradient, and Na^{+}- Cl^{-} in wells farther along the flow path. At the Ban Nat site, upgradient wells have varying water types, ranging from Ca^{2+}-HCO_3 to Na^{+}- Cl^{-} . This chemistry changes to Na^{+}- K^{+}-Cl^{-}—SO_4^{2-}, downgradient. The wells at Ban Rak Chat are all located very near the underlying Khok Kruat bedrock (Figures 8). The wells at Ban Nat are located further down the flow gradient and farther from the bedrock (Figure 9).

Well	pH	Ca^{2+}	Na^{+}	K^{+}	Mg^{2+}	HCO_3^{-}	Cl^{-}	SO_4^{2-}	SiO_2	Fe
ESU1	4.97	2.77	4.58	0.25	1.63	14.03	NA	NA	20.91	0.18
ESU2/ SPB60	5.6	0.46	6.89	1.69	1.63	52.46	2.78	5.70	35.70	4.16
ESU3	5.17	1.21	3.05	0.72	0.89	9.76	1.23	1.16	15.13	0.43
ESU4	5.07	0.91	1.51	0.70	0.79	10.37	0.62	1.16	14.67	0.08
ESU5	5.02	1.03	3.82	0.96	2.08	18.91	13.94	0.44	21.04	7.20
ESU6	6.54	0.36	3.82	0.97	1.28	120.17	8.63	0.03	11.73	109
ESU7	5.6	1.07	5.35	1.88	2.04	121.39	4.68	5.91	30.11	107
ESU8	6.26	78.99	53.82	3.26	10.44	149.45	63.19	163.02	49.25	12.8
ESU9	5.79	6.57	59.20	2.73	5.11	87.84	97.72	74.88	41.25	36.6
ESU10	5.8	10.95	44.58	1.90	4.87	82.96	68.18	52.30	31.56	0.00
ESU11	5.23	1.26	2.28	1.19	1.78	25.62	6.97	2.30	21.16	3.49
SPB10	5.47	7.66	4.58	1.41	2.38	23.18	9.45	10.86	15.56	0.97
SPB11	5.88	8.46	4.58	1.06	2.22	25.62	9.08	9.72	15.14	0.70
SPB21-1	5.28	4.26	7.66	1.31	2.14	28.06	10.49	20.55	18.10	1.95
SPB30	5.4	0.38	4.58	1.57	1.53	43.92	1.59	9.41	35.13	2.39
SPB40	5.51	1.32	11.51	1.09	2.07	42.7	14.70	28.28	34.65	5.38
SPB50	5.25	0.49	3.82	1.75	1.60	28.06	1.68	4.77	29.16	2.18

Table 1: Data obtained from the 2016 sampling event.

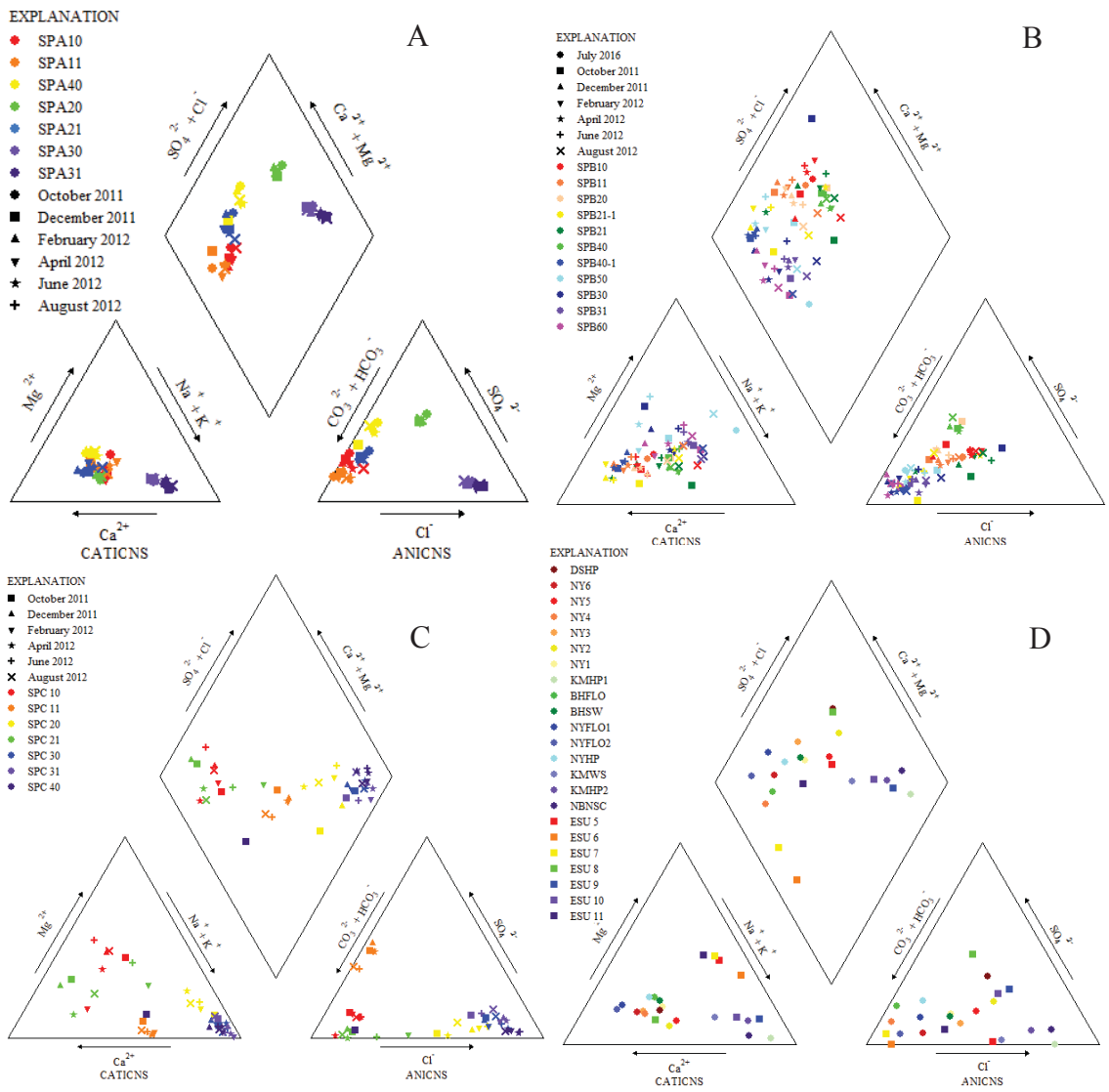

Figure 15: Major ion distributions of the Ban Rak Chat (A) wellsite during the 2011-2012 sampling periods, Ban O Kham (B) wellsite during the 2011-2012 and 2016 sampling periods, Ban Nat (C) wellsite during the 2011-2012 sampling periods, and Ban Dong Sam wellsite (D) during the 2010 and 2016 sampling periods.

4.3 Parameters Measured in the Field during the 2016 Sampling Period

Temperature, pH, oxidation-reduction potential (ORP), electrical conductivity and dissolved oxygen were collected at 19 wells in Ban Haeo, Ban O Kham, and Ban Dong Som, Table 2. Temperatures ranged from 28.80 to 32.45°C with an average of 29.93°C. ORP ranged from -102 to 276 mV with an average value of 148 mV. Most samples have

a positive ORP value indicating the presence of an oxidizing environment. Electrical conductivity ranged from 37 to 957 µS/cm with an average conductance of 186 µS/cm. Dissolved oxygen ranged from -0.08 to 4.66 mg/L with an average concentration of 1.56 mg/L.

	Location	Temperature (°C)	pH	ORP (mV)	EC (µS/cm)	DO (mg/L)
ESU1	Ban Haeo	29.23	4.97	234	71	1.95
ESU2/ SPB60	Ban O Kham	29.18	5.60	102	106	1.17
ESU3	Ban Swang	30.85	5.17	236	44	5.80
ESU4	Ban Swang	30.96	5.07	252	37	3.96
ESU5	Ban Dong Sam	29.67	5.02	276	78	4.66
ESU6	Ban Dong Sam	29.23	6.54	-102	223	0.47
ESU7	Ban Dong Sam	29.44	5.60	66	99	0.06
ESU8	Ban Dong Sam	29.38	6.26	-4	957	1.62
ESU9	Ban Dong Sam	28.78	5.79	31	616	0.03
ESU10	Ban Dong Sam	30.14	5.80	39	444	0.11
ESU11	Ban Dong Sam	28.80	5.23	165	62	-0.08
SPB10	Ban O Kham	31.81	5.47	240	105	1.95
SPB11	Ban O Kham	32.45	5.88	197	79	3.74
SPB20	Ban O Kham	29.76	5.62	254	95	2.56
SPB21-1	Ban O Kham	29.70	5.28	266	105	0.31
SPB30	Ban O Kham	28.66	5.40	155	103	0.07
SPB31	Ban O Kham	29.19	5.47	133	86	0.36
SPB40	Ban O Kham	29.38	5.51	118	161	0.55
SPB50	Ban O Kham	32.05	5.25	155	67	0.39
Average		29.93	5.52	148	186	1.56

Table 2: A multiparameter sonde was utilized to collect field information during the 2016 sampling period.

4.3.1 pH

pH values increase from mid- to downgradient wells at the Ban O Kham wellsite represented by 2011-2012 data as seen in Figure 15 (Thana Thoranee Co. Ltd., 2013). The lowest pH values, generally seen in midgradient wells SPB40 and SPB50, are located farther from the Khok Kraut bedrock (Figure 9). The pH ranged from 4.97 to 6.54

with an average pH value is 5.52. The pH values generally were lowest during rainy season, the months of June and August, and became slightly more alkaline during the dry season as seen in Figure 15. The 2016 data, indicated as the black curve in Figure 7, demonstrate a similar trend in mid- and downgradient wells but upgradient wells are more acidic conditions than observed in the 2011-2012 sampling periods. The 2016 data, indicated as the black curve in Figure 16, demonstrate a similar trend in mid- and downgradient wells but upgradient wells are contain lower pH values than observed in the 2011-2012 sampling period.

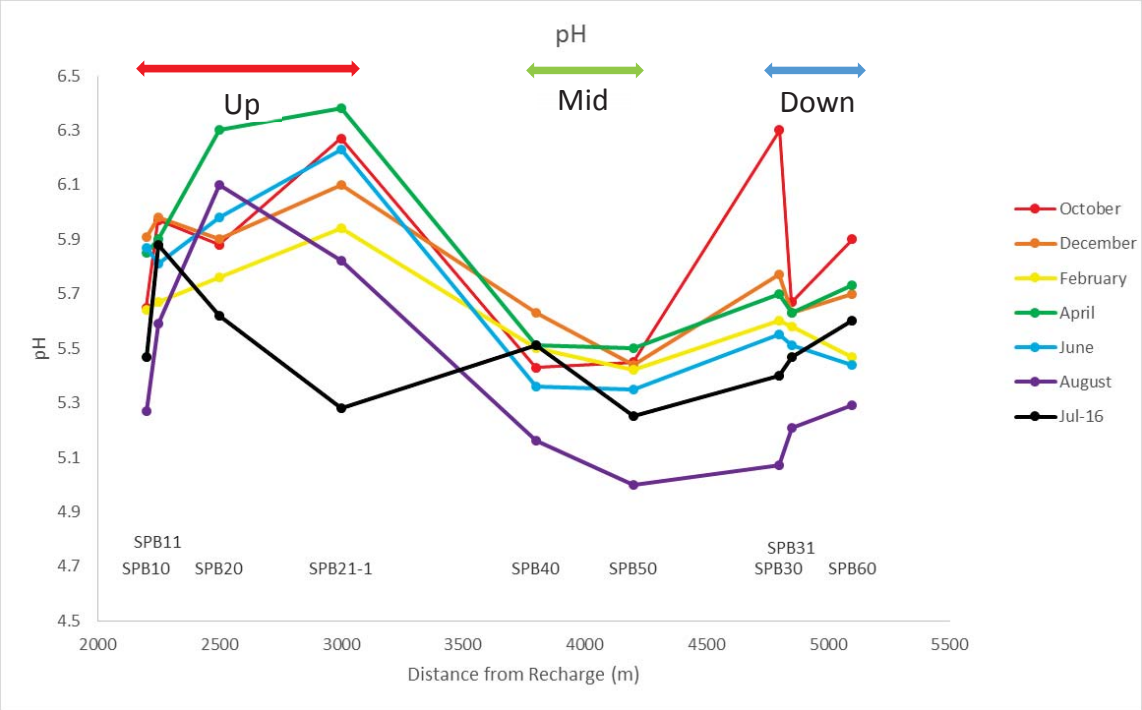

Figure 16: pH variations as the water along a proposed flow path at the Ban O Kham wellsite.

4.4 Alkalinity and pH at Ban O Kham

A comparison of alkalinity and pH was completed to determine if the alkalinity impacts the pH at different locations in the aquifer system. Samples collected during the 2011-2012 sampling periods (Appendix A) and in 2016 (Appendix C) were used in this

interpretation. Groundwater closest to the underlying bedrock formation is likely influenced by alkalinity, based on observations of high alkalinity values in wells located near the bedrock formations.

4.4.1 Alkalinity

Alkalinity was compared seasonally and along the proposed flow path at the Ban O Kham wellsite (Figure 17). Temporal variability is observed in all wells. The highest seasonal variability occur in well SPB21-1 which is the closest well to the underlying bedrock. The lowest alkalinity values are recorded in wells that are further from the Khok Kruat bedrock.

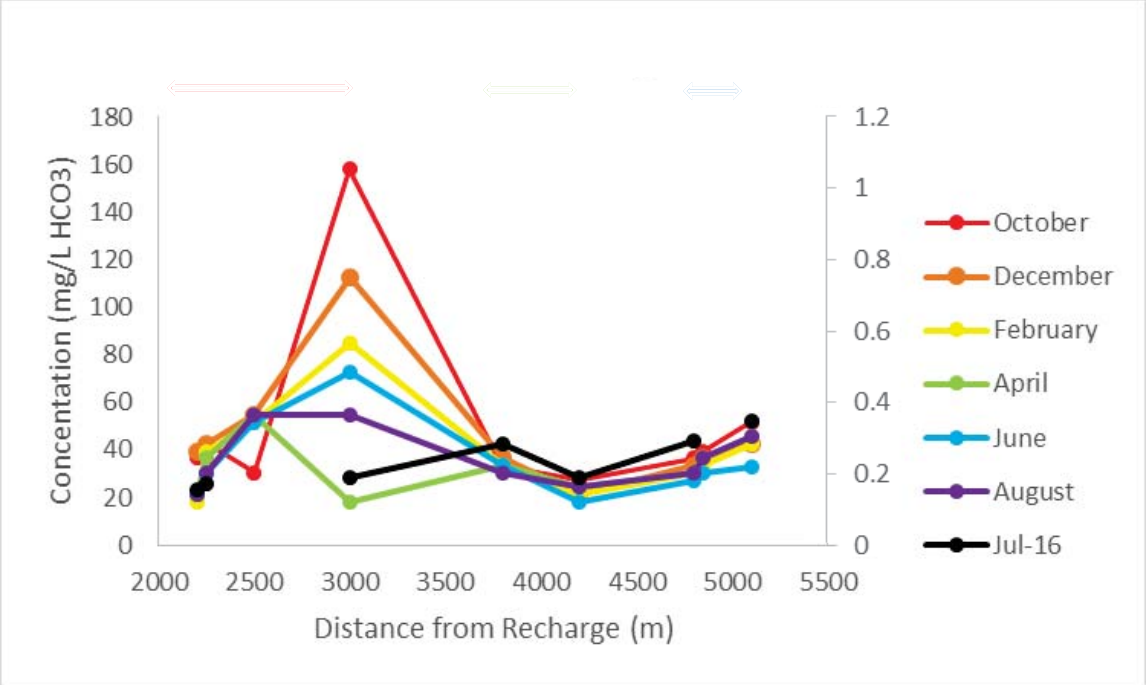

Figure 17: Alkalinity (mg/L HCO3) in the Ban O Kham wells during the 2011-2012 and 2016 sampling periods.

4.4.2 Alkalinity and pH

The relationship between alkalinity and pH was examined in all wells (Figure 18). The highest alkalinity is observed in samples with the highest pH.

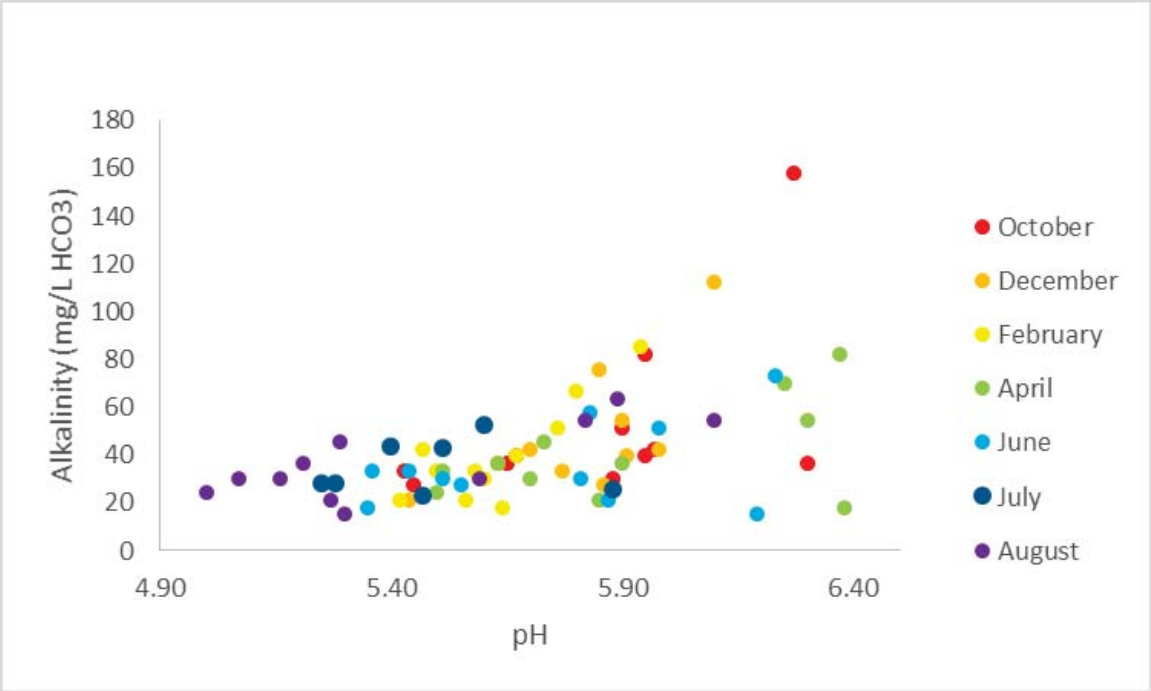

Figure 18: Alkalinity (mg/L HCO3) and pH in all wells during 2011-2012 sampling period.

4.5 Dissolved Silica Concentrations at Ban O Kham

The silica concentrations obtained in July 2016 ranged from 11.73 to 49.25 mg/L SiO_2 with the highest concentrations in downgradient wells (Table 2). The average concentration of dissolved silica was 25.90 mg/L. These values were used to determine saturation indices for silica minerals found in the terrace deposits using PHREEQC (Parkhurst and Apello, 2013). Data from the Ban O Kham wellfield and the 2016 sampling period were used in the analyses. (Thana Thoranee Co. Ltd., 2013). Saturation indices were calculated for crystalline quartz, polycrystalline chalcedony, and amorphous silica in Figure 20 A-C. These values can be seen in Appendix F.

CHAPTER 5: INTERPRETATIONS

5.1 Geochemical Analysis

Results of the chemical analysis on major ions and silica indicate variations in different locations of the aquifer system. The temporal changes were dependent on amount of rainfall that occurred around the sampling event, observed in Figure 5, as well as the spatial changes that are reliant on distance of the well from the underlying bedrock. These are discussed below.

5.1.1 Validation of chemical analyses of July 2016 samples

Validation of laboratory methods was conducted for samples obtained during the summer of 2016. Values for about half of the data for the 2016 sampling event failed to pass the data validation analysis (Appendix F). Though this may be due to the system being out of equilibrium or the cations and anions being out of balance, it is more likely due to laboratory and sampling error as all data from the 2011-2012 sampling periods passed the data validation assessment. Examination of individual parameters suggests that the error may have resulted from erroneous calcium analysis, as calcium values were significantly lower in 2016 than in 2011-2012 sampling events. Errors in field measurements may have also be related to poor calibration of field instruments, as discussed in Appendix B.

The sampling event at Ban O Kham was characterized by drier months than seen when previous data was collected. This resulted in lower alkalinity concentrations and may have contributed to the difference in pH trend seen in upgradient wells.

5.1.2 Major Ion Distributions

Analysis of the piper diagrams from the Ban O Kham, Ban Rak Chat, Ban Dong Sam, and Ban Nat study locations indicate a change in the water chemistry as the water moves along the proposed flow paths for each site, though, the chemistry differs at each wellsite. The differences are likely contributed to the positions of the wells within the groundwater system as wells closer to the underlying bedrock contain higher concentrations of calcium, sodium, potassium, bicarbonate, sulfate, and chloride.

The well nearest to the underlying bedrock at the Ban O Kham wellsite, SPB 21-1, is an upgradient well that has a water chemistry that differs from the other upgradient wells. This well is probably influenced by fluctuations in rainfall that cause dissolution of the Khok Kruat Formation. During the October 2011 sampling period, the highest concentrations for all major ions were reported. The high values may be attributed to the higher precipitation that occurred in months prior to the sampling date. The 2016 sampling data for alkalinity displayed lower alkalinity values that the 2011 and 2012 values, likely due to the dry conditions that occurred prior to the sampling period.

5.2 Field Parameters

Field parameters (Table 1) suggest a transition from oxidizing to reducing conditions along the flowpath. Oxidation-reduction potential decreases in downgradient wells at both field sites indicating more reducing conditions in deeper parts of the system. Increased iron and manganese concentrations in downgradient wells at Ban O Kham, as well as the presence of dark black sediment in this portion of the aquifer from data obtained by the DGR (Thana Thoranee Co. Ltd., 2013), also occur. Lower dissolved

oxygen concentrations are also indicated in the down-gradient wells that in the up-gradient wells.

The electrical conductivity values are generally similar along the proposed flow path, at Ban O Kham, but increased in wells further from the recharge location at the Ban Dong Sam wellsite. This may be due to the intrusion of brine water from salt bearing formations in the bedrock at this wellfield.

The groundwater temperature generally decreases along the proposed flow path at the Ban O Kham and Ban Dong Sam well sites. Temperatures of wells near the recharge area were near the air temperature of around 32°C (Worldwide Weather, 2017).

5.3 Low pH at the Ban O Kham Study Site

The pH values observed at the Ban O Kham wellsite are likely influenced by the buffering of the underlying bedrock formation, the Khok Kruat. Low pH values may exist in the system due to the formation of silicic acid during the dissolution of silica minerals as the spike in silica concentration from up- to mid-gradient wells corresponds to the drop in pH value.

A comparison of alkalinity and pH (Figure 18) indicates an increase in pH as alkalinity increases, possibly due to the pH buffering capacity of calcareous zones that have been documented in the underlying Khok Kruat Formation. As indicated in Figure 17, a decrease in alkalinity is observed in midgradient wells and wells furthest from bedrock. The lower alkalinity suggests that there is a lack of a pH buffering capacity in terrace sediments that are not near the underlying strata.

5.4 High Dissolved Silica at the Ban O Kham Study Site

Dissolved silica concentrations observed at the site are similar to those noted previously (Schulmeister et al. 2015). They are highest in the deepest parts of the terrace deposits and are likely the result of the weathering of the several different silica-bearing materials that are present in the sediments. To evaluate their origin, variations in groundwater Silica concentrations were analyzed using 2011-2012 data for the Ban O Kham study site to analyze seasonal and gradient trends. Silica concentrations increased along the proposed flow path. In 2011-1012, downgradient wells varied more seasonally than upgradient wells did (Figure 19). Seasonal and gradient concentrations are demonstrated in Figure 14 for past and recent data.

The relationship between silica and pH trends was examined in Figure 20. As silica concentrations increase significantly from up- to midgradient wells, pH values demonstrate a sharp decrease. As the water moves to downgradient wells, the pH and silica trend are similar as they both rise.

The saturation indices for three forms of silica materials generally increased down the flow path for amorphous silica rocks, polycrystalline chalcedony, and crystalline quartz. The increase of the saturation indices indicates an increase of the saturation of the groundwater with respect to dissolved silica. Amorphous silica rocks have negative saturation indices in all wells indicating the undersaturation and conditions for dissolution of these silica materials in the system. The presence of tektites in the system suggests that amorphous silica is contributing to the increased silica concentrations present in parts of the system. The conditions for dissolution exist in upgradient wells and precipitation in mid- and downgradient wells for polycrystalline minerals. The abundance

of polycrystalline silica, such as chert and petrified wood, suggests that this form of silica is also contributing to the overall dissolved silica concentration. Crystalline quartz is has a positive saturation index value in all wells down the flow gradient as it is nearly insoluble in natural conditions. This suggests that the crystalline quartz present in the system is not a contributor.

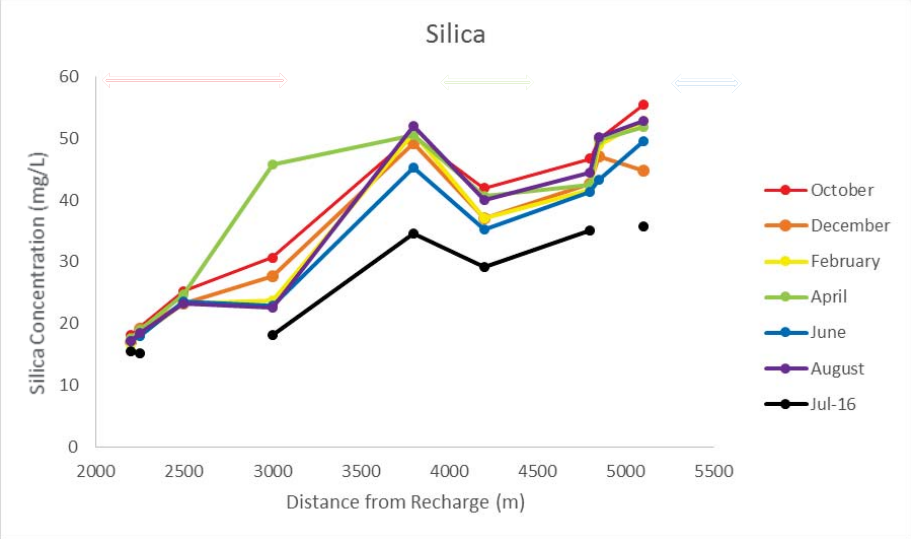

Figure 19: Silica concentrations in wells along the proposed flowpath

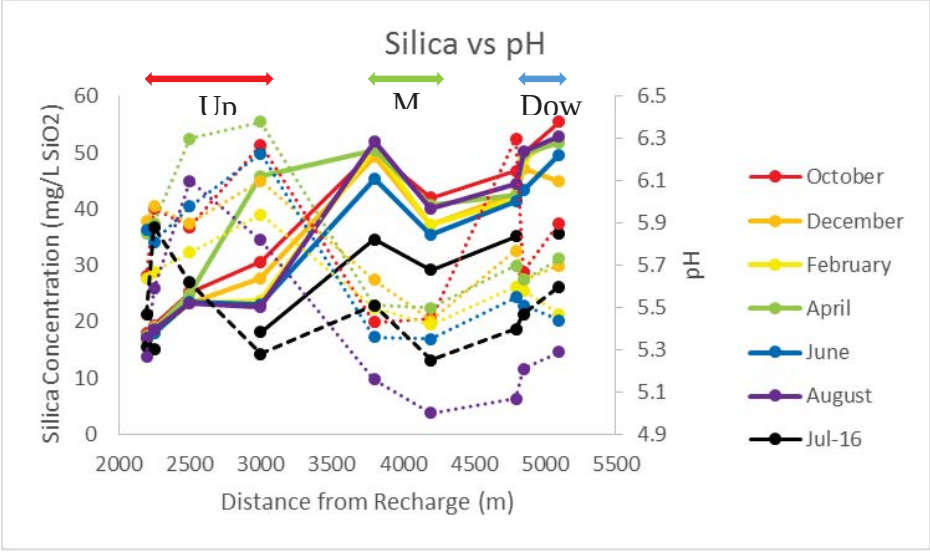

Figure 20: Silica concentration trend, solid lines, and pH value trend, dashed lines, as the waters moves along the flow path.

A

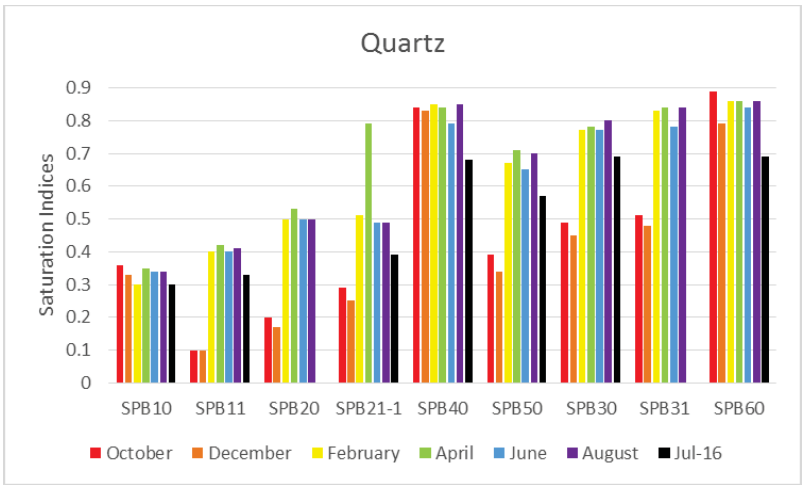

B

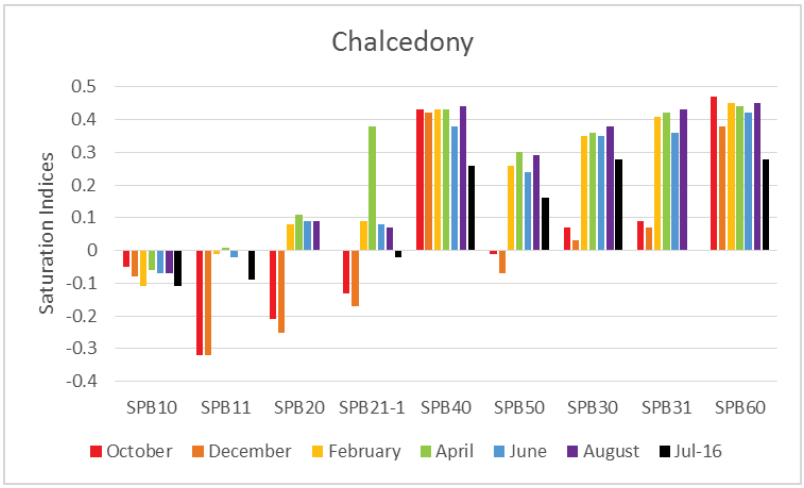

C

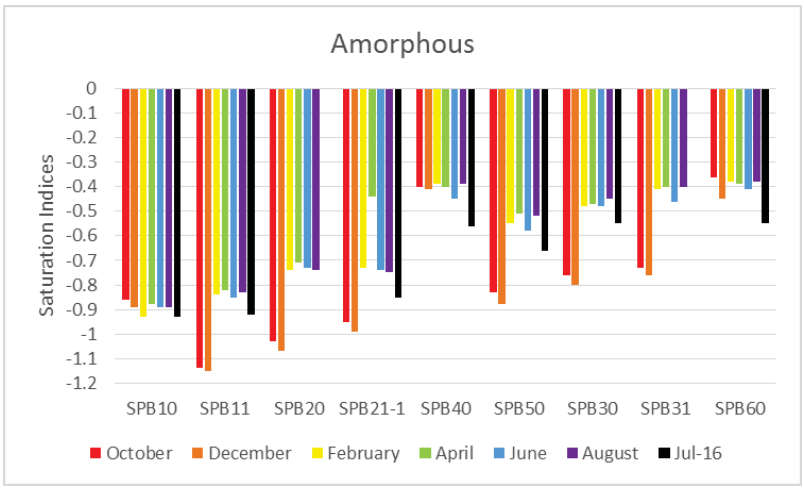

Figure 21: Saturation Index values for A) Crystalline Silica, B) Polycrystalline Chalcedony, and C) Amorphous Silica.

5.5 Ban Rak Chat, Ban Nat, and Ban Dong Sam

Silica and pH trends differ greatly at the Ban Rak Chat and Ban Nat well sites. This difference may be attributed to the locations of the wells in the system, though, further investigation is necessary as there is a limited amount of data from these locations. Similar trends in alkalinity values are observed when investigating alkalinity in the system as wells located most closely to the underlying bedrock resulted in high alkalinity concentrations.

Lack of information on the underlying aquifer system at the Ban Dong Sam make it difficult for analysis. The distribution of major ions showed little to no trend. In order to determine additional information about these well locations, more sampling is necessary.

CHAPTER 6: CONCLUSIONS

The primary purpose of this research was to determine if silica-bearing materials (amorphous, polycrystalline, and crystalline silica) found in Quaternary terrace sediments in the Chi River Basin contributed to high silica concentrations and low pH found in groundwater. Spatial and temporal variations in major ions, silica, and pH were analyzed throughout the terrace gravel groundwater system in order to observe variations in the water as it moved along a proposed flow path. The saturation states of the three silica species were examined to determine if the different species impacted the dissolved silica present in groundwater. Dissolved silica and pH variations along the flow path were compared to determine whether the low pH and high dissolved silica concentrations were related. Results indicate that silica dissolution of amorphous and polycrystalline silica resulted in the increased silica concentrations as well as the formation of silicic acid which lowered the pH of the system at the Ban O Kham wellsite.

Groundwater samples were taken from Ban O Kham during July of 2016 for comparison to earlier data from 2011-2012. The samples taken in 2016 showed a similar trend in dissolved silica concentrations when compared to the 2011-2012 data though the concentrations during the later sampling period were lower. The alkalinity and pH trends were similar for all sampling dates, with a variance in alkalinity concentration and in pH in well SPB21-1, the well located most near the underlying bedrock formation. Samples were also taken from Ban Dong Sam, Ban Haeo, and Ban Sawang though not enough data was available for a thorough analysis of this region.

Field and laboratory data were utilized to determine the saturation index values of crystalline quartz, polycrystalline chalcedony, and amorphous silica in the wells down the

flow path at Ban O Kham, the six sample dates in 2011-2012, and the new data from 2016. Saturation index values range from 0.89 to -1.15 in all collected samples. The dissolution of polycrystalline silica appears to occur in up gradient wells, though the waters become oversaturated as they move downgradient. The waters are oversaturated with respect to quartz at all locations in the system. These results may be a result of the dissolution of silica-rich tektites.

The pH in the system appears to be impacted by the underlying Khok Kruat formation. In wells located in close proximity to the bedrock formation, the pH appears to have been buffered by alkalinity contributed by the calcareous beds in the sedimentary bedrock. In wells farthest from the bedrock (mid-gradient wells) the pH values were the lowest, while silica concentrations were highest in the wells lying closest to the underlying bedrock, suggesting that the low pH is a result of silicic acid formation from silica dissolution.

Further research may be done on the Ban Rak Chat, Ban Nat, and Ban Dong Sam study locations. Obtaining well logs from Ban Dong Song for sampled wells provide information on the components of the subsurface to help determine how the alluvial aquifer may act at this location. Examining the trends observed when analyzing chemical data of the Ban Rak Chat and Ban Nat well sites may provide further insight to the results of this study to determine if the aquifer underlying these locations acts in a similar fashion to the underlying aquifer of Ban O Kham.

Determining locations in the groundwater system where pH is low and dissolved silica concentrations are high can be beneficial to individuals and companies who utilize the waters for domestic and industrial purposes. Increased silica concentrations can cause

scaling on machinery while low pH values can cause corrosion of pipes. Corrosion of pipes can introduce toxic metals into the waters. The importance of knowing which locations in the system produce waters of the best quality is essential for health and industrial purposes.

REFERENCES

American Public Health Association (APHA), American Water Works Association, Water Environment Federation, 1998. Standard methods for the examination of water and wastewater, 20th Ed. Washington, D.C.

Aqion, 2017. Mineral Solubility and Saturation Index. < http://www.aqion.de/site/168> Accessed April 2017.

Environmental Protection Agency, 1974. Method 310.2: Alkalinity (Colorimetric, Automated, Methyl Orange) by Autoanalyzer.

Fetter, C. W., 2001. Applied Hydrogeology, 4th Ed. Prentice-Hall, Upper Saddle River, New Jersey. p. 363.

Fox, E., 2016. Thailand hit by its worst drought in decades. Al Jarzeera. 30 March 2016. Print.

Hach Company, 2005. DR/2400 Spectrophotometer Procedure Manual. Loveland, Co: Hach Company.

Haines, P.W. and Burrett, C., 2004. Flood deposits penecontemporaneous with ~0.8 Ma tektite fall in NE Thailand: Impact-induced environmental effects?. Earth and Planetary Science Letters 205. p. 19-28.

Haworth, H., Javanphet. C.J., and Chaingmai, P.N., 1959. Report on Ground Water Exploration and Development of the Khorat Plateau Region. Royal Department of Mines, Groundwater Bulletin No. 1. Bangkok.

Haworth, H., Chaingmai, P.N., and Phiancharoen, C., 1966. Ground Water Resources Development of Northeastern Thailand. Groundwater Division, Department of Mineral Resources Ministry of National Development, Ground Water Bulletin No. 2. Bangkok.

In-Situ Inc., 2009. Multi-Parameter TROLL 9500 Operator's Manual. Fort Collins, Colorado.

Jayakumar, R., and Lee, E. 2017. Climate Change and groundwater conditions in the Mekong Region- A review. Journal of Groundwater Science and Engineering. vol. 5. no. 1.

Krauskopf, K.B., 1959. The Geochemistry of Silica in Sedimentary Environments. The Society of Economic Paleontologists and Mineralogists. p. 4-19.

LaMoreaux, P., Charaljavanaphet, C., N. Jalichan, P.P.M Cheingmai, Bunnag, D., Thavisri, A., Rathpakthm, C., 1958, Reconnaissance of the Geology and Groundwater of

the Khorat Plateau, U.S. Geological Survey Water Supply Paper 1429, U.S. Government Printing office, Washington, D.C.

Lenntech, 2016, Silicon and Water. Water Treatment Solutions. Accessed 4 June 2016. http://www.lenntech.com/periodic/water/silicon/silicon-and-water.htm

McFarland, M.L., Provin, T.L., Boellstorff, D.E., 2008, Drinking Water Problems: Corrosion, Texas A&M Agrilife Extension.

Morris, S., 1989. Lambda 2 UV/VIS Spectrometer Operator's Manual. Perkin Elmer. Federal Republic of Germany.

National Drought Mitigation Center, 2017. ENSO and Drought Forecasting. University of Nebraska-Lincoln.

Parkhurst, D.L., and Appelo. C.A.J., 2013. Description of Input and Examples for PHREEQC Version 3- A Computer Program for Speciation Batch-Reaction, One-Dimensional Transport, and Inverse Geochemical Calculations. United States Geological Survey.

Pidwirny M., and Jones, S., 2015. Physical Geography. Climate Classification and Climatic Regions of the World. <http://www.physicalgeography.net/fundamentals/7v.html> Accessed April 2017

Pradeep, K., Nepolian, M., Anandhan, P., Kaviyarasan, R., Prasanna, M.V., and Chidambaram, S. 2016. A study on variation in dissolved silica concentration in groundwater of hard rock aquifers in Southeast coast of India. Materials Science and Engineering. 121.

Ridd, M.F., Barber, A.J., and Crow, M.J., 2011. The Geology of Thailand. The Geological Society. London.

Royal Meteorology Department, 2015. online data: http://www.tmd.go.th/ retrieved March 3, 2016.

Saminpanya, S. and Sutherland, F.L., 2013. Silica phase-transformation during diagenesis within petrified woods found in fluvial deposits from Thailand-Myanmar. Sedimentary Geology vol. 209. p. 15-26.

Schulmeister, M., Lertsirivorakul, R., Nettasana, T., and Assiri, P., 2015. Hydrogeochemistry of the Flowing Artesian Wellfield of the Northern Khorat Plateau, Northeastern Thailand, In: Proceedings GEOINDO 2015 Khon Kaen,Thailand, (ISBN 978-616-223-143-8)

Tarbuck, E.J. and Lutgens, F.K., 2015, Earth Science: Custom Edition for Emporia State

University, 4th edition. Pearson, Boston, MA p. 47.

Thana Thoranee, Co. Ltd., 2013. Sustainable Development of Flowing Artesian well field in Central Chi River Basin, Project, Executive Summary. A report to the Thailand Ministry of Natural Resources and Environment, Department of Groundwater Resources. pp. 44. Phutthamonthon, Nakhon Pathom.

United States Geological Survey, 2016, Standard Reference Sample Project. USGS Branch of Quality Systems. Accessed 4 June 2016. https://bqs.usgs.gov/srs/

Varian, 1999, Cary 50 Operation Manual. Walnut Creek, CA. Publication 50, No. 85

Winston, R.B., 2000, Graphical User Interface for MODFLOW, Version 4. United States Geological Survey. Open Report: 00-315.

Wongsawat, S., Dhanesvanich,O., and Panjasutaros, P., 1992. Groundwater Resources of Northeastern Thailand, Department of Mineral Resources. Bangkok.

Worldwide Weather Online, 2017. Khon Kaen. Accessed 4 April 2017. https://www.worldweatheronline.com/khon-kaen-weather-averages/khon-kaen/th.aspx

Yongdong, W., Zhang, W., Shaolin, Z., Jintasakul. P., Grote. P.J., and Boonchai, N., 2006, Recent advances in the study of Mesozoic-Cenozoic petrified wood from Thailand. Progress in Natural Science. vol. 16. no. 5. p. 501-506

APPENDIX A- pH, major Ion, Iron, and Dissolved Silica concentrations- A Summary of DGR Chemical Data

Well	pH	Ca^{2+}	Na^{+}	K^{+}	Mg^{2+}	HCO_3^{-}	Cl^{-}	SO_4^{2-}	SiO_2	Fe
SPA10	5.88	12.00	12.07	0.65	4.87	66.88	1.18	19.51	33.50	0.98
SPA11	5.86	11.20	8.05	0.95	2.44	57.76	0.39	7.06	24.87	0.38
SPA20	6.93	126.00	113.80	4.60	20.81	191.52	129.39	297.47	61.16	3.11
SPA21	6.02	37.60	19.54	2.15	6.36	121.60	12.94	43.63	37.57	1.07
SPA30	6.04	19.20	51.73	1.95	4.88	45.60	87.83	19.45	32.70	5.54
SPA31	5.78	17.60	64.37	2.55	4.88	48.64	104.30	17.63	29.64	4.20
SPA40	6.00	52.80	25.29	4.35	16.59	161.12	12.94	110.31	60.64	1.22
SPB10	5.65	13.60	6.90	1.15	2.45	36.48	7.84	15.81	18.05	0.30
SPB11	5.97	15.20	3.45	1.30	2.45	42.56	6.27	11.63	19.32	0.22
SPB20	5.88	10.40	9.20	2.50	3.41	30.40	9.02	24.29	25.22	1.97
SPB21-1	6.27	40.00	19.54	5.85	3.94	158.08	24.70	3.05	30.65	2.30
SPB30	6.30	4.00	6.32	1.55	2.92	36.48	3.14	2.65	46.74	2.19
SPB31	5.67	4.80	7.47	1.50	2.92	39.52	3.92	4.00	49.93	2.61
SPB50	5.45	5.60	4.60	1.40	2.92	27.36	5.49	5.69	41.97	4.59
SPB60	5.90	5.60	10.35	1.90	3.41	51.68	3.92	4.06	55.48	7.46
SPB40	5.43	10.40	9.20	1.90	3.41	33.44	9.02	22.31	50.43	4.60
SPC10	6.04	2.40	2.87	0.15	1.95	18.24	1.57	2.35	13.78	0.13
SPC11	6.09	21.60	34.49	1.80	0.51	82.08	3.53	53.38	33.08	0.48
SPC20	5.71	1.60	6.90	1.35	1.95	15.20	10.59	0.62	13.62	0.20
SPC21	5.45	8.00	1.72	0.90	2.44	33.44	3.92	1.06	14.62	0.03
SPC30	5.42	1.60	25.86	0.80	0.97	15.20	32.15	6.32	14.46	0.75
SPC31	5.10	0.80	15.52	1.15	0.97	12.15	18.04	4.25	13.51	0.10
SPC40	6.06	14.40	24.71	1.50	2.93	97.28	12.55	3.63	10.41	0.68

Table 1: pH and concentrations (mg/L) from October 2011 sampling period.

Well	pH	Ca^{2+}	Na^{+}	K^{+}	Mg^{2+}	HCO_3^{-}	Cl^{-}	SO_4^{2-}	SiO_2	Fe
SPA10	6.34	15.20	13.79	1.20	3.42	72.96	1.18	17.80	31.55	0.76
SPA11	6.22	11.20	6.90	0.50	2.93	54.72	1.57	8.01	25.41	0.61
SPA20	6.58	112.80	95.41	3.50	16.18	203.68	104.69	235.47	55.64	0.14
SPA21	6.80	28.80	17.24	1.45	5.38	109.44	8.23	31.44	35.18	0.38
SPA30	6.19	20.80	52.88	1.85	5.86	54.72	90.58	17.86	28.66	6.16
SPA31	5.44	17.60	71.27	2.20	3.91	45.60	114.50	16.63	27.76	4.92
SPA40	6.00	36.00	20.69	3.40	12.19	148.96	4.71	56.25	50.15	2.39
SPB10	5.91	12.00	6.90	1.50	1.96	39.52	6.27	11.75	16.92	0.73
SPB11	5.98	16.80	3.45	1.25	2.94	42.56	8.23	11.88	19.10	0.82
SPB20	5.90	19.20	8.05	1.30	3.43	54.72	9.80	19.69	23.18	11.2
SPB21-1	6.10	33.60	6.90	1.20	3.44	112.48	7.46	9.75	27.69	3.41
SPB30	5.77	5.60	2.30	1.60	2.92	33.44	0.78	3.38	42.71	1.93
SPB31	5.63	5.60	6.90	0.85	2.92	36.48	4.31	4.63	47.07	2.68
SPB50	5.44	4.00	1.15	1.25	3.41	21.28	5.10	3.56	37.15	1.36
SPB60	5.70	8.00	3.45	1.45	2.93	42.56	0.39	5.56	44.84	4.58
SPB40	5.63	12.00	11.50	0.70	2.93	36.48	7.45	23.44	49.23	4.57
SPC10	6.70	4.80	2.30	1.50	3.41	30.40	3.92	3.49	13.97	1.57
SPC11	7.02	17.60	32.19	1.10	0.51	69.92	2.35	51.99	30.61	0.37
SPC20	5.28	1.60	26.44	1.20	1.46	36.86	36.86	3.85	13.48	0.05
SPC21	5.50	8.00	1.15	0.40	1.95	33.44	3.14	1.22	14.45	0.06
SPC30	4.94	2.40	26.44	0.60	1.46	18.24	35.68	5.87	14.16	0.17
SPC31	4.88	0.80	26.44	0.30	0.97	9.12	34.11	5.69	14.07	0.22
SPC40	5.50	6.40	63.22	1.10	1.95	27.36	96.06	6.24	15.82	0.37

Table 2: pH and concentrations (mg/L) from December 2011 sampling period.

Well	pH	Ca^{2+}	Na^{+}	K^{+}	Mg^{2+}	HCO_3^{-}	Cl^{-}	SO_4^{2-}	SiO_2	Fe
SPA10	5.62	12.80	11.50	1.80	2.45	66.88	0.78	14.41	30.26	1.58
SPA11	5.68	9.60	8.05	1.30	1.96	48.64	1.57	8.29	25.42	0.59
SPA20	6.21	116.00	85.06	2.90	19.58	200.64	108.22	237.84	57.05	0.64
SPA21	6.60	29.92	12.64	2.10	5.19	103.36	8.63	32.25	36.68	0.76
SPA30	6.28	16.00	45.98	2.30	4.39	45.60	73.71	15.38	28.09	0.30
SPA31	5.75	17.60	64.37	3.40	2.94	42.56	103.12	15.38	27.71	2.55
SPA40	6.00	36.00	17.24	2.70	12.19	121.60	7.84	72.82	68.57	2.23
SPB10	5.64	9.60	4.02	1.20	1.96	18.24	9.80	9.91	16.70	0.34
SPB11	5.67	15.20	4.60	1.40	2.45	39.52	9.80	11.59	18.05	0.34
SPB20	5.76	17.60	5.75	1.00	3.42	51.68	8.23	18.86	23.23	1.67
SPB21-1	5.94	25.60	3.45	1.70	4.41	85.12	7.84	11.41	23.73	8.83
SPB30	5.60	4.80	4.60	1.10	1.95	30.40	1.57	3.82	41.75	1.72
SPB31	5.58	4.80	6.90	1.00	2.92	33.44	5.49	3.76	48.95	2.73
SPB50	5.42	4.80	1.15	1.80	1.46	21.28	1.57	3.45	37.10	2.37
SPB60	5.47	8.00	5.17	1.00	2.44	42.56	1.96	3.70	52.84	6.02
SPB40	5.50	10.40	11.50	1.60	2.44	33.44	9.02	22.85	50.99	4.86
SPC10	6.07	6.40	2.87	1.00	0.98	25.84	2.35	3.15	14.10	1.50
SPC11	6.56	17.60	34.49	1.00	0.99	76.00	4.71	50.79	30.14	0.76
SPC20	4.70	1.60	13.79	0.45	1.46	12.16	20.00	1.82	13.67	0.19
SPC21	4.83	2.40	4.60	0.50	1.46	15.20	6.27	0.36	13.64	0.42
SPC30	4.94	2.40	33.34	1.20	1.46	21.28	44.70	4.79	14.70	0.89
SPC31	4.72	0.80	28.74	0.40	0.97	12.16	37.25	5.33	14.27	0.41
SPC40	5.08	3.20	52.88	1.00	0.98	18.24	75.28	5.03	14.89	1.47

Table 3: pH and concentrations (mg/L) from February 2012 sampling period.

Well	pH	Ca^{2+}	Na^{+}	K^{+}	Mg^{2+}	HCO_3^{-}	Cl^{-}	SO_4^{2-}	SiO_2	Fe
SPA10	6.03	12.80	11.50	0.80	1.96	60.80	2.35	13.60	30.95	0.36
SPA11	5.96	6.80	7.47	1.20	2.44	48.60	1.18	6.20	25.62	0.33
SPA20	6.64	116.00	93.10	3.60	17.15	206.70	109.00	243.00	55.72	0.25
SPA21	6.65	19.20	10.35	1.70	4.88	79.00	5.49	20.20	30.44	0.34
SPA30	6.60	14.40	41.40	1.20	4.88	42.60	66.70	14.80	28.06	0.28
SPA31	5.85	12.80	49.40	1.40	4.39	39.50	80.00	11.70	25.57	1.75
SPA40	6.03	33.60	21.80	2.00	11.70	121.60	7.84	68.60	66.50	2.32
SPB10	5.85	9.60	4.00	1.10	1.96	21.30	9.00	8.90	17.57	0.17
SPB11	5.90	12.80	4.60	0.65	2.45	36.50	7.80	9.10	18.96	0.13
SPB20	6.30	17.60	9.20	0.60	3.40	54.70	9.00	20.00	24.76	0.84
SPB21-1	6.38	5.60	5.75	0.70	2.40	18.20	9.40	8.50	45.82	0.16
SPB30	5.70	4.80	4.60	0.90	1.95	30.40	1.57	1.57	42.51	1.90
SPB31	5.63	4.80	6.90	0.50	2.92	36.50	5.50	2.10	49.70	2.71
SPB50	5.50	4.80	1.15	1.10	2.44	24.30	1.96	2.60	40.70	3.42
SPB60	5.73	6.40	5.17	1.60	2.92	45.60	1.96	1.80	51.86	5.97
SPB40	5.51	10.40	11.50	1.40	2.44	33.40	9.40	21.20	50.51	4.52
SPC10	6.17	4.00	2.30	0.10	1.95	24.30	1.60	0.30	14.43	0.92
SPC11	6.84	19.20	34.50	0.35	0.50	76.00	5.10	50.50	30.05	0.10
SPC20	5.67	1.60	9.20	0.70	1.95	15.20	12.90	0.40	14.04	0.01
SPC21	6.03	13.60	4.60	0.65	1.50	51.70	5.50	0.00	14.70	0.02
SPC30	5.50	1.60	56.30	1.00	2.40	21.30	79.60	6.30	16.45	0.70
SPC31	5.33	0.80	25.30	0.60	1.50	9.10	35.70	5.20	14.87	0.31
SPC40	5.40	2.40	43.70	1.10	1.50	12.20	65.90	2.83	14.79	0.23

Table 4: pH and concentrations (mg/L) from April 2012 sampling period.

Well	pH	Ca^{2+}	Na^{+}	K^{+}	Mg^{2+}	HCO_3^{-}	Cl^{-}	SO_4^{2-}	SiO_2	Fe
SPA10	6.44	14.40	12.64	1.10	2.93	69.92	3.92	13.33	28.41	0.08
SPA11	5.91	8.80	8.62	0.35	2.44	48.64	3.14	6.37	25.12	0.07
SPA20	6.44	116.00	93.11	2.50	19.58	203.68	112.53	248.54	54.81	0.08
SPA21	6.63	19.20	12.64	0.80	4.40	79.04	5.88	20.99	30.00	0.09
SPA30	6.54	13.60	39.08	1.10	3.90	36.48	61.56	14.27	26.98	0.36
SPA31	5.93	12.80	50.92	0.95	4.88	42.56	94.10	14.50	26.55	3.73
SPA40	5.97	32.00	21.84	2.00	10.73	118.56	10.19	64.33	63.34	2.12
SPB10	5.87	9.60	4.02	0.60	2.44	21.28	8.63	10.12	17.18	0.07
SPB11	5.81	12.00	4.60	0.30	2.93	30.4	8.63	10.00	17.92	0.06
SPB20	5.98	18.40	11.50	0.70	2.94	51.68	12.94	17.89	23.50	0.72
SPB21-1	6.23	24.80	6.90	0.70	2.46	72.96	10.19	13.63	22.97	1.25
SPB30	5.55	4.00	4.60	0.30	2.92	27.36	3.14	5.20	41.42	0.80
SPB31	5.51	4.00	5.17	0.90	2.92	30.4	3.14	3.86	43.32	2.13
SPB50	5.35	3.20	1.15	0.40	2.92	18.24	2.74	3.16	35.34	2.41
SPB60	5.44	4.00	5.17	1.00	3.41	33.14	1.96	3.22	49.57	4.26
SPB40	5.36	9.60	11.50	0.60	4.39	33.44	9.80	23.27	45.28	5.27
SPC10	6.01	3.20	1.15	0.60	2.43	21.28	2.74	2.40	13.96	0.57
SPC11	6.50	20.00	34.49	0.10	1.00	91.2	3.53	39.77	28.91	0.12
SPC20	5.62	1.60	14.94	0.80	1.95	15.2	30.58	3.16	13.66	0.11
SPC21	5.49	2.40	3.45	0.80	1.95	15.2	3.53	0.06	13.35	0.09
SPC30	5.28	1.60	51.73	0.00	1.46	15.2	49.01	5.61	12.49	0.19
SPC31	5.13	0.80	13.79	0.30	0.97	9.12	18.82	4.27	13.58	0.18
SPC40	5.22	4.00	56.33	0.80	1.95	15.2	87.05	4.50	12.58	0.74

Table 5: pH and concentrations (mg/L) from June 2012 sampling period.

Well	pH	Ca^{2+}	Na^{+}	K^{+}	Mg^{2+}	HCO_3^{-}	Cl^{-}	SO_4^{2-}	SiO_2	Fe
SPA10	6.55	14.40	12.64	1.70	2.93	63.84	6.67	13.37	26.60	0.10
SPA11	5.90	9.60	8.62	1.00	1.96	48.64	2.35	6.14	24.58	0.24
SPA20	7.86	116.00	93.11	5.90	19.58	203.68	111.75	257.75	56.33	0.08
SPA21	6.20	17.60	13.79	1.90	4.40	79.04	5.88	21.52	30.19	0.13
SPA30	5.96	12.80	33.34	2.20	3.90	36.48	54.89	13.08	26.41	0.34
SPA31	5.36	13.60	60.92	1.90	3.90	39.52	94.10	16.29	27.85	2.41
SPA40	5.81	36.00	21.84	3.20	13.17	127.68	5.49	78.05	68.36	2.40
SPB10	5.27	9.60	5.75	1.40	1.47	21.28	9.80	10.46	17.13	0.09
SPB11	5.59	12.80	4.60	1.00	2.45	30.40	9.80	10.94	18.54	0.06
SPB20	6.10	16.80	9.20	1.10	3.42	54.72	8.63	18.36	23.28	0.36
SPB21-1	5.82	18.40	6.90	1.30	2.45	54.72	10.19	14.04	22.60	0.80
SPB30	5.07	4.00	8.05	1.20	2.43	30.40	7.06	4.98	44.47	1.54
SPB31	5.21	4.80	8.62	1.30	2.44	36.48	5.88	4.74	50.31	2.67
SPB50	5.00	4.00	2.87	1.50	2.43	24.32	1.96	4.74	39.96	3.50
SPB60	5.29	4.80	6.90	1.30	3.89	45.60	1.57	4.44	52.90	5.90
SPB40	5.16	9.60	9.20	1.70	2.93	30.40	6.27	23.71	52.00	4.45
SPC10	5.95	3.20	1.72	1.70	2.43	21.28	2.35	2.31	13.94	0.21
SPC11	7.00	24.00	34.49	1.20	1.49	103.36	0.78	48.15	28.55	0.15
SPC20	5.21	2.40	14.94	1.90	1.95	18.24	18.82	3.53	14.15	0.90
SPC21	5.50	5.60	2.87	0.00	1.49	27.36	2.35	0.43	13.50	0.09
SPC30	4.67	1.60	26.44	0.80	0.49	12.16	34.50	6.75	14.52	0.20
SPC31	4.57	0.80	13.79	1.20	0.97	6.08	18.04	4.74	13.77	0.26
SPC40	5.52	5.60	77.02	0.20	1.95	33.44	106.65	6.44	13.31	2.47

Table 6: pH and concentrations (mg/L) from August 2012

APPENDIX B: Calibration of Field Analytical Equipment

A Troll 9500 Multiparameter Sonde (In-Situ Inc., 2009) was calibrated for pH, electrical conductivity, and oxidation-reduction potential at the Geotechnology laboratory at Khon Kaen University before and after all samples were collected. In-Situ Inc.'s Quick Cal solution is temperature dependent and was utilized for calibration (Table 1). The initial calibration for pH utilized pH standard solutions at pH values 4 and 7 as well as the Quick Cal solution. Oxidation-reduction potential and electrical conductivity were calibrated using the Quick Cal Solution, Table 2, at a temperature of 30°C. The dissolved oxygen probe was not calibrated due to lack of calibration solution.

Temperature (°C)	pH	ORP (mV)	EC (µS/cm)
5	7.10	255	4990
10	7.04	247	5690
15	7.03	239	6450
20	7.02	231	7160
25	7.00	224	8000
30	6.98	217	8830
35	6.97	209	9690
Standard Deviation	±0.02	±5	±40

Table 1: Quick Calibration values are dependent on the temperature of the calibration solution. Table from the QuickCal solution bottle.

	Initial (Quick Cal at 15°C)	Final (Quick Cal at 30°C)
pH- 4 Solution	4	4.15
pH- 7 Solution	7	7.04
pH- Quick Cal	7.03	7.05
EC- Quick Cal	6450 µS/cm	5634 µS/cm
EC- 1413 µS/cm	1413 µS/cm	1202 µS/cm
ORP- Quick Cal	239 mV	200 mV

Table 2: Calibration verification before and after field measurements were made.

Final calibration for pH showed little drifting of the instrument using pH solutions and the Quick Cal solution sensor which indicates that data on all samples is valid. For ORP, the Quick Cal solution was used at a temperature of 30°C was to give a reading of

217 mV. The value from the instrument was 200 mV indicating a drift of 17 mV. Electrical conductivity at 30°C was to give a reading of 8830 µS/cm using the Quick Cal solution. The reading was very low at 5634 µS/cm. A second calibration was completed using a 1413 µS/cm standard solution. The instrument gave a reading of 1202 suggesting a higher drift in more conductive solutions. Due to the low EC values obtained on the groundwater samples, it is likely that most of the data is of acceptable quality. Due to the inability to calibrate the dissolved oxygen sensor, the quality of the data is unknown and can only be used for relative purposes.

APPENDIX C: Calibration Curves for Major Ions, Iron and Dissolved Silica

Calibration curves (Figure 1 A-G), were created using known standard solutions to find concentrations of calcium, sodium, magnesium, potassium, chloride, and sulfate in groundwater samples. Samples outside of the calibration range were diluted with deionized water. Major ion and dissolved silica concentrations can be viewed in Table 1. Alkalinity values were reported from the titration analysis. Calibration curves were made and can be viewed in Appendix G. The calcium calibration curve had a range from 0-30 mg/L with samples ranging from 0.38 to 78.99 mg/L. The sodium calibration curve had a range of 0-100 mg/L with samples ranging from 1.51 to 59.20 mg/L. The magnesium calibration curve ranged from 0-5 mg/L with samples falling in the range of 0.79 to 10.44 mg/L. The potassium calibration curve ranged from 0-2 mg/L with groundwater samples having a concentration range from 0.25 to 3.26 mg/L. For chloride, the calibration curve ranged from 0-100 mg/L with sample concentrations in the range of 0.62 to 97.72 mg/L. The sulfate calibration curve, ranging from 0-100 mg/L, yielded sample concentrations in the range of 0.03 to 163.02 mg/L. The alkalinity analysis produced results in the range of 9.76 to 149.45 mg/L HCO_3^-.

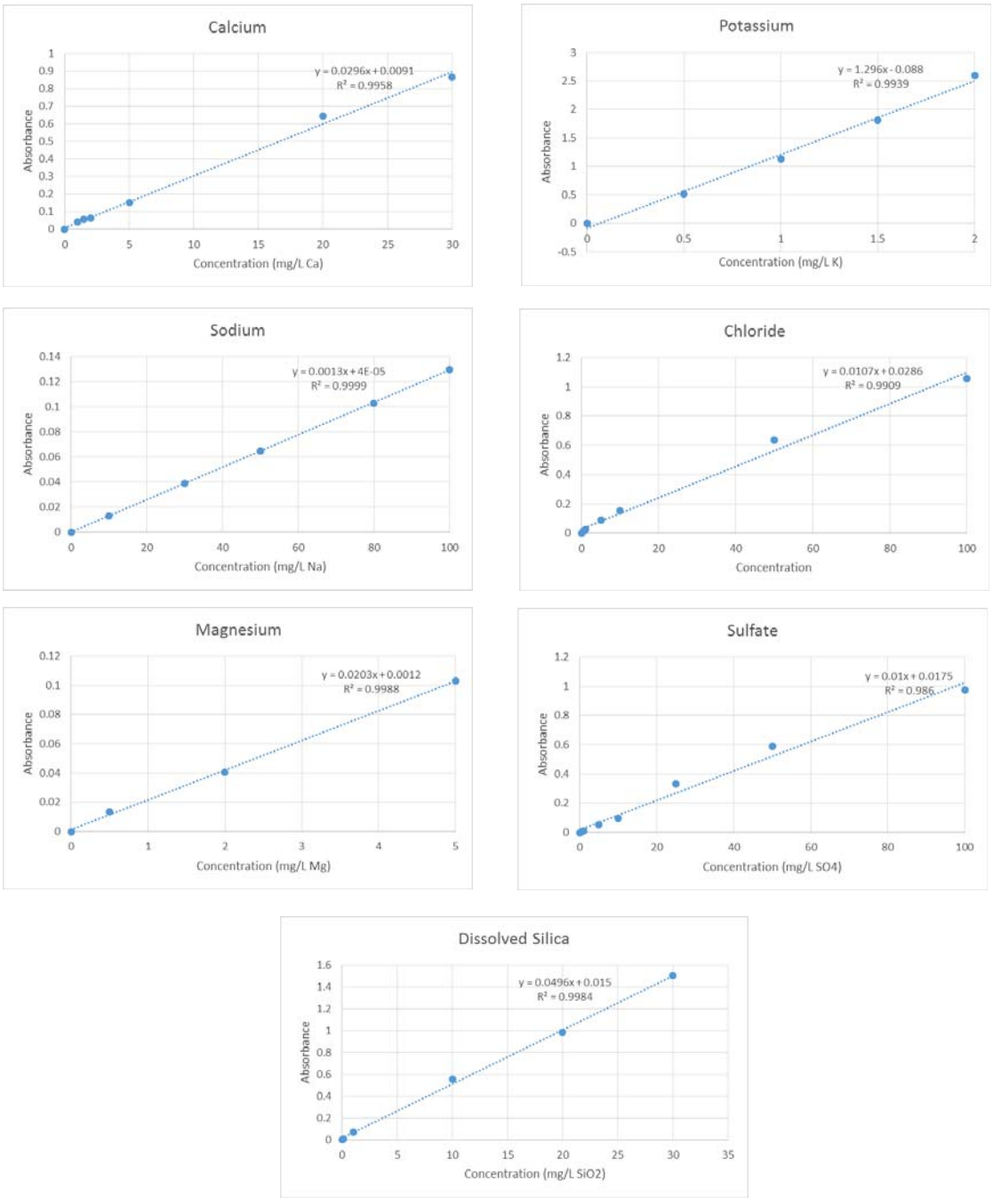

Figure 1: Calibration Curves for Laboratory Data. A) Calcium, B) Potassium, C) Sodium, D) Chloride, E) Magnesium, F) Sulfate, G) Dissolved Silica

APPENDIX D: Laboratory Analytical Equipment at Khon Kaen University laboratory

Figure 1: Filtration system utilized in the laboratory analysis.

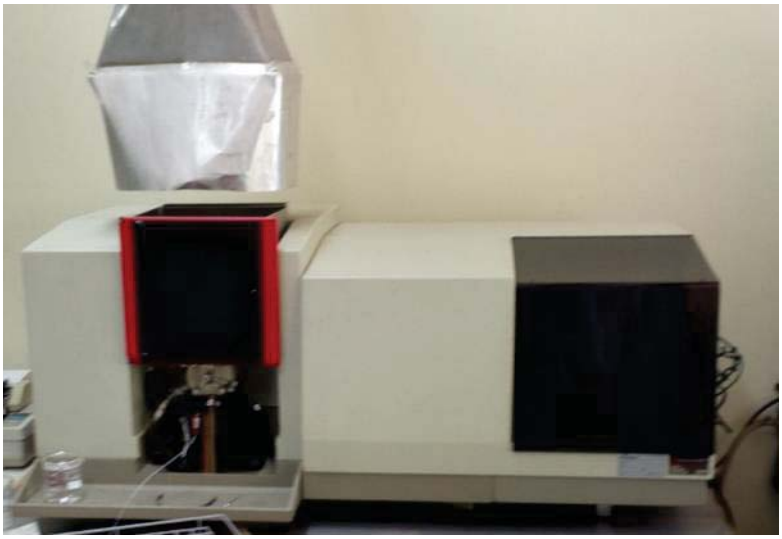

Figure 2: Flame atomic absorption spectrometer used to determine major ion and iron analysis.

Figure 3: Lambda 2 UV-VIS Spectrophotometer utilized for analysis at wavelength 390 nm.

Appendix E- Validation of Dissolved Silica in Groundwater Measurements using the Molybdosilicate Method and two ESU-owned, UV-Vis Spectrophotometers

The field based nature of this research project requires the use of portable analysis of dissolved silica in groundwater. The use of pre-measured reagents and a field spectrophotometer would greatly aid in the determination of dissolved silica. To determine if a pre-measured reagent version of the EPA molybdosilicate method, method 370.1, could be used reliabily, the method was used to meausre known concentration samples on field and lab sprectrophotometers (APHA, 1998). The Hach DR/2400 Portable Spectrophotometer (Hach, 2002) and the Varian Cary 50 UV-Vis Spectrophotometer (Varian, 1999) are compared in this appendix.

INTRODUCTION

Background

The U.S. Geological Survey (USGS) conducts an inter-laboratory comparison study semiannually (USGS, 2016). The Standard Reference Sample Project provides a variety of Standard Reference Samples (SRSs) for laboratory quality assurance testing that are available to purchase by laboratories wishing to conduct internal quality control on specific methods. Samples are prepared bi-annually and test sample categories include trace metals, major ions, nutrients, ionic-strength, and mercury. The majority of samples are prepared with water from Colorado streams and spiked with reagent grade chemicals to measurable concentrations. Three USGS samples were provided to ESU by the Kansas Geological Survey (KGS) for this evaluation. Sample numbers M214, M216, and M218, major ion constituent samples, were used for analysis for this report.

To identify an accepted concentration for each sample, the round robin test samples are analyzed at approximately 40 professional laboratories around the country using inductively coupled plasma, inductively coupled plasma/mass spectroscopy, and

colorimetric methods with the most precise results from the colorimetric method which utilizes a spectrophotometer. The results were compiled to find the average concentration and concentration ranges of silica in each sample (Table 1) (USGS, 2016).

	Concentration (mg/L SiO_2)	**Concentration Ranges (mg/L SiO_2)**
M218	24.1	10.60-26.15
M216	15.1	6.28-17.05
M214	9.18	4.60-11.00

Table 1**:** Silica Concentrations of Reference Standards.

METHODS

In the silicomolydbate method, silica and phosphate in the sample will react with molybdate ions, from sodium molydbate reagent, in low pH conditions, formed by sulfamic acid reagent, to form yellow silicomolydbic acid complexes and phosphomolybdic acid complexes. The addition of the citric acid reagent destroys the phosphate complexes (Hach, 2002). To provide a portable analytical method that may be used for field analysis, Hach Company ™ created pre-measured reagents in the form of powder filled pillows. Powder pillows are premeasure reagents designed for the alaysis of 10 mL samples and a spectrophotometer.The powder pillows utilized for this method include sodium molybdate, sulfamic acid, and citric acid (Hach 2002).

The Hach method was designed for evaluation of samples using a Hach DR/2400 Portable Spectrophotometer. The DR/2400 interally loaded program # 656 (High Range Silica) is examined in this evaluation, with a wavelength of 452 nm. 10 mL of sample is placed in a round sample cell. The sodium molybdate powder pillow (Molydbate Reagent, Catalog #21073-69) is added and the solution is swirled to dissolve the reagent completely. The sulfamic acid reagent (Acid Reagent, Catalog #21074-69) is added to

solution and swirled to mix. A 10 minute reaction period is enforced in which a yellow color will develop if silica or phosphate are present. The citric acid powder pillow (Citric Acid, Catalog #21062-69) is added after the reaction period and the solution is swirled to mix. A two minute reaction period is enforced. Another round sample cell is filled with 10 mL of sample to run as a blank. The blank is placed into the sample cell holder and the "Zero" button is selected to display a zero absorbance. The prepared sample is placed into the sample cell holder and the "Read" button is selected (Hach, 2002). Samples are run three times and absorbance values are recorded.

To allow for comparison of concentrations measured using the Hach 2400 with the ESU laboratory based Varian Cary unit, samples were run on both units consecutively. Immediately after the samples are run through the Hach spectrophotometer, approximately 1 mL of the prepared sample is placed in a 1 cm cuvette to run on the Varian Cary 50 UV-Vis Spectrophotometer. Another 1 cm cuvette is filled with origonal sample to run as a blank. The blank sample is placed into the sample holder and run to create a zero baseline. The prepared sample is placed into the sample holder. The wavelength range utilized is 300-600 nm. Each sample was analyzed one time on the instrument. Data is collected at a 0.67 nm interval and scanned for 0.1375 seconds (Varian, 1999). Since no peak was present to indicate where the instrument is the most sensitive, different wavelengths were analyzed to find the wavelength which produced the most accurate results. Wavelength 390 nm was utilized as results were within 2% of known concentrations. Other wavelengths analyzed were 375 nm, 380 nm, 395 nm, 400 nm, 410 nm, and 452 nm.

RESULTS

Standards were made from a 1000 mg/L SiO_2 stock solutions. Seven standards were made at 1 mg/L, 15 mg/L, 25 mg/L, 35 mg/L, 50 mg/L, 75 mg/L, and 100 mg/L. The published linear range for the Hach instrument is 1-100 mg/L (Hach, 2002). The linear range for the Cary unit was unknown. The standards were analyzed using the portable Hach spectrophotometer and the Cary UV-Vis spectrophotometer to create calibration curves (Figures 19 and 20). Both calibration curves show linear data within the linear ranges, 1-100 mg/L, of the instrument.

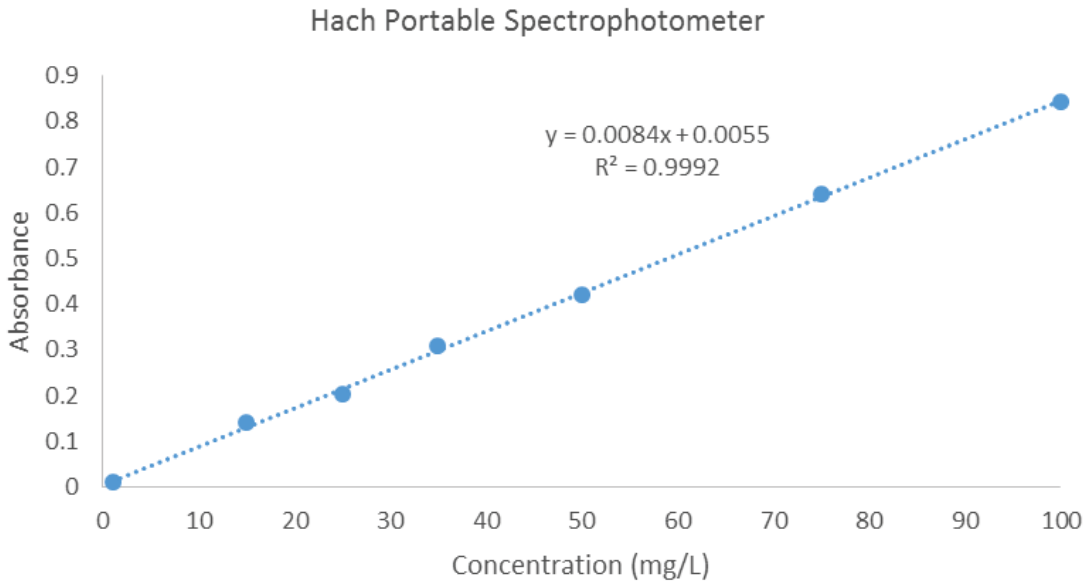

Figure 1: Calibration curve utilizing the Hach Portable Spectrophotometer.

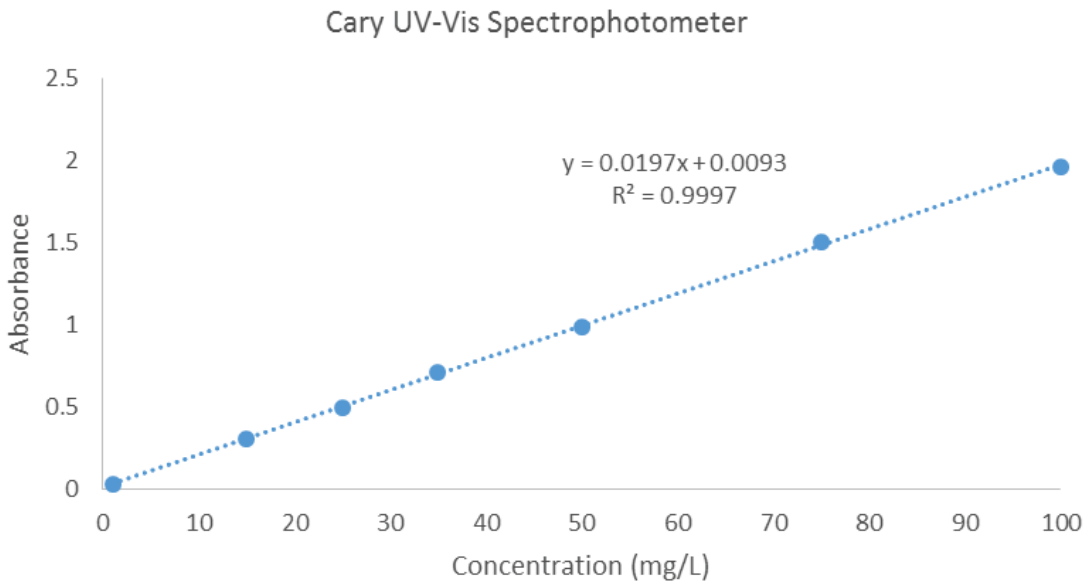

Figure 2: Calibration curve utilizing the Cary UV-Vis Spectrophotometer.

The USGS standards were analyzed using both spectrophotometers to determine if concentrations compare to USGS values. The standards were analyzed and concentrations were calculated from absorbance values using Beer's Law. Three replicates were evaluated on the Hach spectrophotometer to determine the precision of the instrument. The standard deviation was within the width of the symbols in Figures 18 and 19.

	Hach Concentration (mg/L SiO_2)	**Standard Deviation**	**Cary Concentration (mg/L SiO_2)**	**USGS Concentration (mg/L)**	**Standard Deviation**
M218	23.15	0.11	23.59	24.1	3.01
M216	15.77	0.07	15.34	15.1	1.65
M214	9.58	0.13	9.15	9.18	1.12

Table 2**:** Comparison of Hach and Cary concentrations with values obtained from USGS.

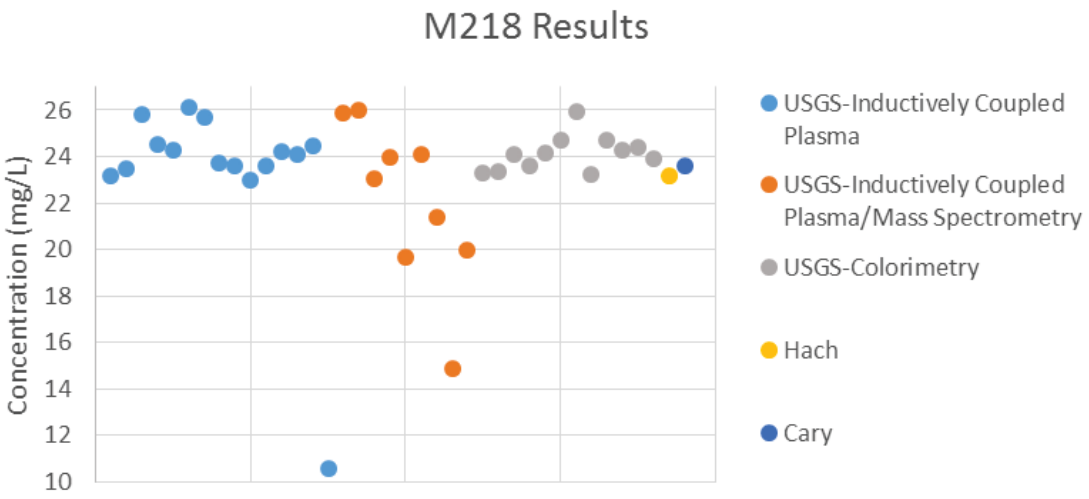

Figure 3: Comparison of the Hach and Cary Spectrophotometers to other methods for M218.

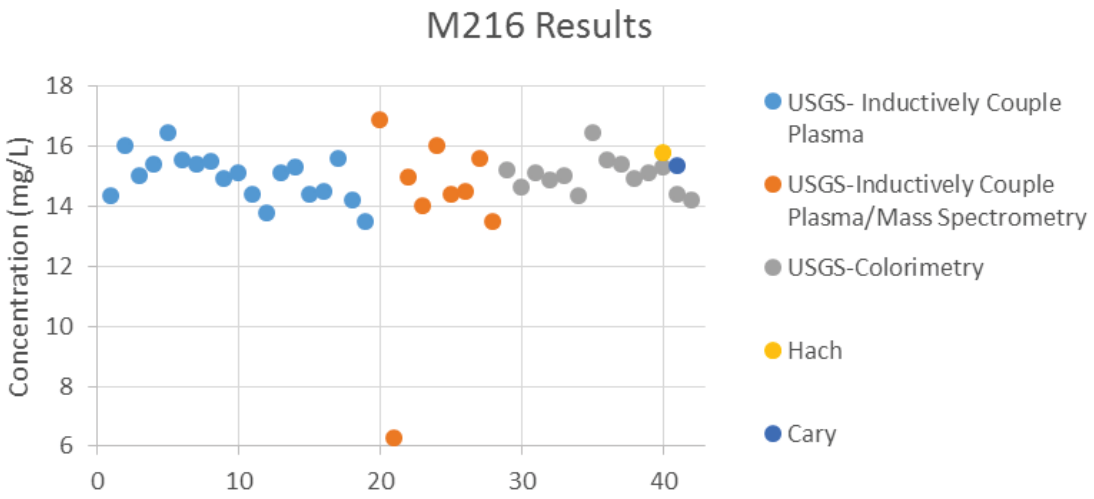

Figure 4: Comparison of the Hach and Cary Spectrophotometers to other methods for M216.

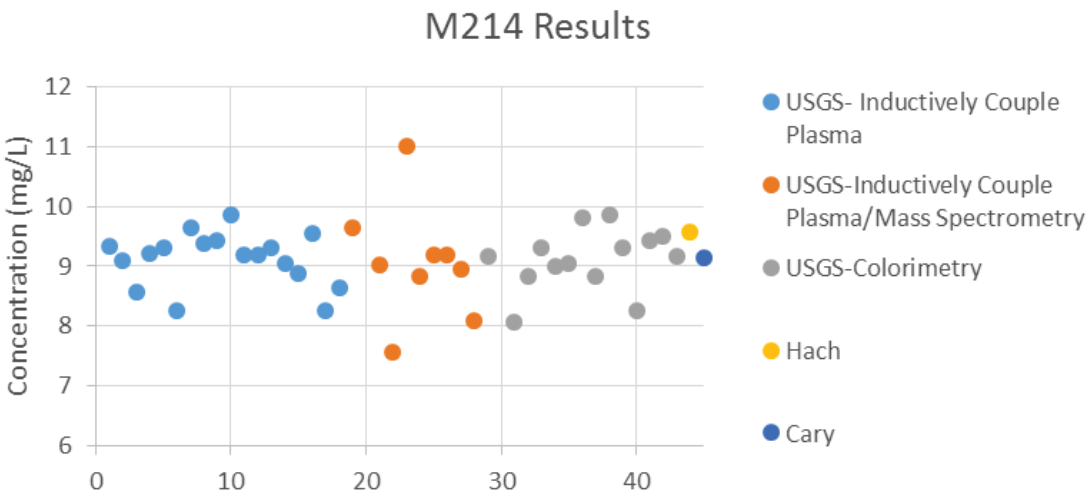

Figure 5: Comparison of the Hach and Cary Spectrophotometers to other methods for M214.

CONCLUSION

Both spectrophotometers produced data comparable to the USGS values, with each sample falling within the round robin range, using Hach's silicomolybdate method. The Cary spectrophotometer produced values more similar to the reported USGS values (Table 2). Since each sample was only analyzed one time on the Cary spectrophotometer, the standard deviation cannot be reported. The Cary spectrophotometer produced more accurate results with a percent difference range of 0.32-2.11%. The Hach portable spectrophotometer produced reliable data that was less accurate than the Cary instrument with a percent difference range of 3.94-4.44%.

Appendix F- Saturation Index Values

	Chalcedony	Quartz	Amorphous
SPB10	-0.05	0.36	-0.86
SPB11	-0.32	0.1	-1.14
SPB20	-0.21	0.2	-1.03
SPB21-1	-0.13	0.29	-0.95
SPB40	0.43	0.84	-0.4
SPB50	-0.01	0.39	-0.83
SPB30	0.07	0.49	-0.76
SPB31	0.09	0.51	-0.73
SPB60	0.47	0.89	-0.36

Saturation index values for the October 2011 sampling date.

	Chalcedony	Quartz	Amorphous
SPB10	-0.08	0.33	-0.89
SPB11	-0.32	0.1	-1.15
SPB20	-0.25	0.17	-1.07
SPB21-1	-0.17	0.25	-0.99
SPB40	0.42	0.83	-0.41
SPB50	-0.07	0.34	-0.88
SPB30	0.03	0.45	-0.8
SPB31	0.07	0.48	-0.76
SPB60	0.38	0.79	-0.45

Saturation index values for the December 2011 sampling date.

	Chalcedony	Quartz	Amorphous
SPB10	-0.11	0.3	-0.93
SPB11	-0.01	0.4	-0.84
SPB20	0.08	0.5	-0.74
SPB21-1	0.09	0.51	-0.73
SPB40	0.43	0.85	-0.39
SPB50	0.26	0.67	-0.55
SPB30	0.35	0.77	-0.48
SPB31	0.41	0.83	-0.41
SPB60	0.45	0.86	-0.38

Saturation index values for the February 2012 sampling date.

	Chalcedony	Quartz	Amorphous
SPB10	-0.06	0.35	-0.88
SPB11	0.01	0.42	-0.82
SPB20	0.11	0.53	-0.71
SPB21-1	0.38	0.79	-0.44
SPB40	0.43	0.84	-0.4
SPB50	0.3	0.71	-0.51
SPB30	0.36	0.78	-0.47
SPB31	0.42	0.84	-0.4
SPB60	0.44	0.86	-0.39

Saturation index values for the April 2012 sampling date.

	Chalcedony	Quartz	Amorphous
SPB10	-0.07	0.34	-0.89
SPB11	-0.02	0.4	-0.85
SPB20	0.09	0.5	-0.73
SPB21-1	0.08	0.49	-0.74
SPB40	0.38	0.79	-0.45
SPB50	0.24	0.65	-0.58
SPB30	0.35	0.77	-0.48
SPB31	0.36	0.78	-0.46
SPB60	0.42	0.84	-0.41

Saturation index values for the June 2012 sampling date.

	Chalcedony	Quartz	Amorphous
SPB10	-0.07	0.34	-0.89
SPB11	0	0.41	-0.83
SPB20	0.09	0.5	-0.74
SPB21-1	0.07	0.49	-0.75
SPB40	0.44	0.85	-0.39
SPB50	0.29	0.7	-0.52
SPB30	0.38	0.8	-0.45
SPB31	0.43	0.84	-0.4
SPB60	0.45	0.86	-0.38

Saturation index values for the August 2012 sampling date.

	Chalcedony	Quartz	Amorphous
SPB10	-0.11	0.3	-0.93
SPB11	-0.09	0.33	-0.92
SPB20	0	0	0
SPB21-1	-0.02	0.39	-0.85
SPB40	0.26	0.68	-0.56
SPB50	0.16	0.57	-0.66
SPB30	0.28	0.69	-0.55
SPB31	0	0	0
SPB60	0.28	0.69	-0.55

Saturation index values for the July 2016 sampling date.

APPENDIX G- Validation of laboratory methods used to measure chemical parameters in samples obtained during 2011-2012 and 2016 sampling periods

Well	Oct 2011	Dec 2011	Feb 2012	Apr 2012	June 2012	Aug 2012
SPA10	0.06	0.07	-0.03	-0.03	0.00	0.04
SPA11	0.03	0.01	0.01	-0.06	0.01	0.05
SPA20	0.01	0.01	-0.12	-0.18	-0.17	-0.26
SPA21	-0.03	-0.01	-0.09	-0.02	-0.01	-0.02
SPA30	0.01	0.04	0.07	0.06	0.10	0.05
SPA31	0.00	0.03	0.08	0.04	-0.37	0.06
SPA40	0.03	0.04	-0.11	0.00	-0.09	0.04
SPB10	0.02	0.03	0.06	0.05	0.07	0.04
SPB11	-0.02	0.09	0.03	0.05	0.10	0.06
SPB20	0.02	0.04	-0.04	0.01	0.09	0.03
SPB21-1	0.11	0.03	-0.02	0.00	-0.01	0.01
SPB30	0.01	0.02	0.01	0.05	0.01	-0.03
SPB31	0.02	0.03	0.02	0.00	0.02	-0.01
SPB50	0.02	0.00	-0.01	0.01	0.02	0.01
SPB60	0.03	0.00	0.02	-0.01	0.07	0.01
SPB40	0.05	0.06	-0.02	0.00	0.05	0.00
SPC10	0.06	-0.02	0.00	0.01	-0.06	0.00
SPC11	0.03	0.05	0.05	0.07	0.18	0.15
SPC20	0.01	-0.34	0.01	0.04	-0.27	0.03
SPC21	-0.03	-0.04	0.02	0.02	0.08	0.02
SPC30	0.01	-0.02	0.01	0.03	0.71	-0.01
SPC31	0.00	0.05	0.02	0.01	-0.03	0.02
SPC40	0.03	-0.03	0.04	-0.03	0.03	0.21

Table 1: Charge balances for the DGR samples obtained during the 2011-2012 sampling periods.

	Charge Balance	Calculated vs Observed TDS	TDS vs EC
ESU2/ SPB60	-0.56	1.0	2.23
ESU3	0.07	1.0	3.94
ESU4	-0.02	1.0	3.30
ESU5	-0.30	1.2	2.82
ESU6	-1.90	2.3	0.22
ESU7	-1.74	2.0	1.20
ESU8	-0.40	1.7	0.63
ESU9	-2.36	1.7	0.56
ESU10	-1.44	1.6	0.57
ESU11	-0.33	1.0	0.99
SPB10	-0.06	1.2	0.79
SPB11	-0.05	1.2	0.08
SPB21-1	-0.43	1.1	0.86
SPB30	-0.58	1.1	0.96
SPB40	-0.94	1.2	0.92
SPB50	-0.24	0.8	0.96

Table 2: Validation of lab and field data obtained during the 2016 sampling period.

I, Katy Lee Schwinghamer , hereby submit this thesis to Emporia State University as partial fulfillment of the requirements for an advanced degree. I agree that the Library of the University may make it available to use in accordance with its regulations governing materials of this type. I further agree that quoting, photocopying, digitizing or other reproduction of this document is allowed for private study, scholarship (including teaching) and research purposes of a nonprofit nature. No copying which involves potential financial gain will be allowed without written permission of the author. I also agree to permit the Graduate School at Emporia State University to digitize and place this thesis in the ESU institutional repository.

_____

Signature of Author

_____

Date

The Origin of High Silica and Low pH in the Groundwater of the Quaternary Terrace Deposits in the Northern Khorat Basin in Northeastern Thailand

Title of Thesis

_____

Signature of Graduate School Staff

_____

Date Received